

**FREQUENCY REGULATION OF INTERCONNECTED
POWER SYSTEM WITH THE INTRODUCTION OF
COMMUNICATION DELAY IN SMART GRID**

submitted in fulfillment of the requirements for the award of degree of

Master of Engineering
in
Power Systems

Submitted By
Rushil Sagotra
(Roll No. 801642009)

Under the supervision of:

Dr. Manoj Badoni
Assistant Professor
EIED, TIET, Patiala

Dr. Vijay Pratap Singh
Assistant Professor
EED, REC, Sonbhadra



THAPAR INSTITUTE
OF ENGINEERING & TECHNOLOGY
(Deemed to be University)

June 2018

Electrical and Instrumentation Engineering Department
Thapar Institute of Engineering and Technology
Patiala

(Declared as Deemed-to-be-University u/s 3 of the UGC Act., 1956)

Post bag No. 32, Patiala – 147004
Punjab (India)

CERTIFICATE

I hereby certify that the work which is presented in dissertation entitled, "Frequency Regulation of Interconnected Power System with the Introduction of Communication Delay in a Smart Grid", in partial fulfillment of the requirements for the degree of Master of Engineering in Power Systems, submitted to Electrical & Instrumentation Engineering Department of Thapar Institute of Engineering and Technology, Patiala is as authentic record of my own work carried under the supervision of Dr. Manoj Badoni (EIED, TIET) and Dr. Vijay Pratap Singh (EED, REC Sonbhadra). The matter contained in this report has not been submitted, neither in part nor in full to any other degree to any other university or institute except as reported in text and references.

Place: Patiala

Date: 19/7/18

Rushil Sagotra
(Rushil Sagotra)

Roll No.: 801642009

It is certified that the above statement made by the student is correct to the best of my knowledge and belief.

Manoj Badoni

(Dr. Manoj Badoni)

Assistant Professor, EIED

Vijay Pratap Singh

(Dr. Vijay Pratap Singh)

Assistant Professor, EED

Thapar Institute of Engineering and Technology, Rajkiya Engineering College, Sonbhadra, U.P.
Patiala

Countersigned by

(Dr. R S Kaler)

Head (EIED)

Thapar Institute of Engineering and Technology,
Patiala

(Dr. S S Bhatia)

Dean (Academic Affairs)

Thapar Institute of Engineering and Technology
Patiala

ACKNOWLEDGEMENTS

Words are sometimes less to show one's extensive appraise. With this understanding that my work like all this can never be the outcome of a single person. I take this opportunity to express my profound sense of gratitude and respect for all those who helped me through the duration of this work.

I am very thankful to **Dr. Prakash Gopalan**, Director of Thapar Institute of Engineering and Technology, Patiala for providing the potential for the completion of M.E. I manifest my deep sense of gratitude towards **Dr. R S Kaler**, Head of the Department of Electrical & Instrumentation Engineering, Thapar Institute of Engineering and Technology, Patiala and had been persistent origin of creativity for me right through this exertion.

I would like express my gratitude and thanks to supervisor, **Dr. Manoj Badoni**, Assistant Professor, Department of Electrical and Instrumentation Engineering, Thapar Institute of Engineering and Technology, Patiala, and **Dr. Vijay Pratap Singh**, Assistant Professor, Department of Electrical and Instrumentation Engineering, Rajkiya Engineering College, Sonbhadra for his patient guidance and support through this work. It was an honor and privilege to work under him as a student. He also provided help in technical writing and presentation style and I found their guidance to be extremely valuable for me every time.

I am also grateful to my batch mates who devoted their valuable time for the successful completion of dissertation. I extend my gratitude to the researchers and scholars whose hours of toil have produced the papers that I have utilized in my project.

Lastly, I want to extend thank my parents for precious years of unyielding endearment and encouragement. They have always wanted the best for me and admire their determination, hardwork and sacrifice.

(Rushil Sagotra)

(801642009)

ABSTRACT

The aim of load frequency control (LFC) for any power quarter lies only for control of frequency and tie line scheduled power within the confines of acceptable bounds. Presenting restructuring of power territory made us to analyze that standard of power distribution and generation has become the need of hour. The dissertation work includes with control scheme in combination with the PI controller. The tie line power perturbations and the frequency perturbations have been foreshortened due to entanglement of non-exhaustible resources with the traditional two area system have been modeled. The procure with traditional controller staging is compared for working with multiple uncertainty based H_∞ controller and results claimed proved predominant for the proposed control. The remarkable outcome of communication delay has given my model a different perspective in the area of modernized grid. Delaying of signal in the larger system can make sluggish control feedback to the network and may become reason for system power miscarriage. Thus, propound model control finds its culmination ascribed to communication delay. Different specimens have been analyzed for ensuring the robust working of the developed model. The model is considered for different penetrations of vehicle to grid (V2G) contrivance.

Keywords: Load Frequency Control, Proportional Integral, Vehicle to Grid.

TABLE OF CONTENTS

CERTIFICATE	i
ACKNOWLEDGEMENTS	ii
ABSTRACT	iii
TABLE OF CONTENTS	iv
LIST OF FIGURES	vii
LIST OF TABLES	x
LIST OF ABBREVIATIONS	xi
CHAPTER 1	1
INTRODUCTION	1
1.1 Overview	1
1.2 Literature Review	2
1.3 Gaps Identified	6
1.4 Motivation	7
1.5 Objectives	8
1.6 Expected Deliverables	8
1.7 Organization of Thesis Work	8
1.8 Conclusion	9
CHAPTER 2	10
DESIGN AND MODELING OF PROPOSED SYSTEM	10
2.1 Introduction	10
2.2 Modeling of Two Area Power System	11
2.2.1 Linear Thermal Model	12
2.2.2 Linear LFC Model	15
2.2.3 Linear Vehicle Model	16
2.2.4 Wind Power Model	17
2.2.5 Two Area Power System Interconnected By Tie Line	19
2.2.6 Area Control Error	20
2.2.7 Power System Model	20
2.3 Conclusion	23

CHAPTER 3	25
PROPOSED CONTROLLER FOR TWO AREA SYSTEM	25
3.1 Introduction	25
3.2 Design of Controller for Proposed Two Area System	25
3.2.1 Conventional Controller	26
3.2.2 Design of Multiple Uncertainty Based H-Infinity Controller	28
3.2.3 Working of Multiple Uncertainty Based H-Infinity Controller	29
3.3 Conclusion	32
CHAPTER 4	33
MODELING OF TWO AREA POWER SYSTEM WITH COMMUNICATION DELAY	33
4.1 Introduction	33
4.2 System Performance with Communication Delay	34
4.2.1 Incorporating Communication Delay in the System	35
4.2.2 State Space Analysis	36
4.3 Conclusion	42
CHAPTER 5	43
SIMULATION RESULTS AND DISCUSSION	43
5.1 Introduction	43
5.2 System Configuration	44
5.3 Performance of System with Conventional Controller	44
5.3.1 Random Change of Wind Speed for Step Change in load	45
5.3.2 Step Change of Wind Speed for Step Change in load	45
5.3.3 Step Change in Wind Speed with Random Change in load	46
5.4 Performance of System with H_{∞} Controller	48
5.4.1 Random Change of Wind Speed for Step Change in load	48
5.4.2 Step Change of Wind Speed for Step Change in load	51
5.4.3 Step Change of Wind Speed for Random Change in load	54
5.5 Comparison Based on Performance of PI and H_{∞} Controller	55
5.5.1 Random Change of Wind Speed for Step Change in load	55
5.5.2 Step Change of Wind Speed for Step Change in load	55
5.5.3 Step Change of Wind Speed for Random Change in load	56
5.6 Performance of System with Communication Delay	57
5.6.1 Random Change of Wind Speed for Step Change in load	57
5.6.2 Step Change of Wind Speed for Step Change in load	58
5.6.3 Step Change of Wind Speed for Random Change in load	59

5.7 Performance of System with Different Penetration of Electric Vehicle	60
5.7.1 Random Change of Wind Speed for Step Change in load	60
5.7.2 Step Change of Wind Speed for Step Change in load	61
5.7.3 Step Change of Wind Speed for Random Change in load	62
5.8 Performance Indices	63
5.9 Conclusion	64
CHAPTER 6	65
CONCLUSION & FUTURE SCOPE	65
6.1 Conclusion	65
6.2 Future Scope	66
PUBLICATION	67
REFERENCES	68
APPENDIX	73
PLAGIARISM REPORT	78

LIST OF FIGURES

Figure 2.1 Frequency vulnerability	10
Figure 2.2 Generator with basic frequency control	11
Figure 2.3 Basic layout of system	12
Figure 2.4 Transfer function of turbine model	13
Figure 2.5 Transfer function of generator-load model	14
Figure 2.6 Transfer function of governor model	15
Figure 2.7 Transfer function of LFC model	16
Figure 2.8 Transfer function of vehicle model	16
Figure 2.9 Wind power block diagram	18
Figure 2.10 Proposed power system model	20
Figure 3.1 Basic controller	26
Figure 3.2 Proposed PI controller	27
Figure 3.3 Block diagram of H–Infinity controller	28
Figure 3.4 Multiple Uncertainty Based H–Infinity Controller	29
Figure 4.1 System with introduction of communication delay	34
Figure 4.2 State space model of two area interconnected system	36
Figure 5.1 Simulink model developed for smart power system	44
Figure 5.2 Random wind speed given to wind plant	45
Figure 5.3 System frequency response with PI controller with random wind speed	45
Figure 5.4 Step change in wind speed given to system	46
Figure 5.5 System frequency response with PI controller with step wind speed	46
Figure 5.6 System response with random change in load in area 1	47
Figure 5.7 System response with random change in load in area 2	47
Figure 5.8 System response with PI controller with random change in load	47
Figure 5.9 System frequency response with H_{∞} controller with random change in wind speed	48
Figure 5.10 System area control error response with H_{∞} controller with random change in wind speed	48
Figure 5.11 System tie line power response with H_{∞} controller with random change in wind speed	49
Figure 5.12 Power capacity of each unit in area 1 with H_{∞} controller with random change in wind speed	49

Figure 5.13 Power capacity of each unit in area 2 with H_∞ controller with random change in wind speed	50
Figure 5.14 Wind power output (MW) with H_∞ controller with random change in wind speed	50
Figure 5.15 Wind power output (pu) with H_∞ controller with random change in wind speed	50
Figure 5.16 System frequency response with H_∞ controller with step wind speed	51
Figure 5.17 System area control error response with H_∞ controller with step wind speed	51
Figure 5.18 System tie line power response with H_∞ controller with step wind speed	52
Figure 5.19 Power capacity in area 1 with H_∞ controller with step wind speed	52
Figure 5.20 Power capacity in area 2 with H_∞ controller with step wind speed	53
Figure 5.21 Wind power capacity (MW) with uncertainty control with step wind speed	53
Figure 5.22 Wind power capacity (pu) with uncertainty control with step wind speed	53
Figure 5.23 System frequency response with H_∞ controller with random change in load	54
Figure 5.24 System tie line power response with H_∞ controller with random change in load	54
Figure 5.25 System frequency response with comparison of controllers for area 1	55
Figure 5.26 System frequency response with comparison of controllers for area 2	55
Figure 5.27 System frequency response for area 1 with step change in wind speed	55
Figure 5.28 System frequency response for area 2 with step change in wind speed	56
Figure 5.29 System frequency response for area 1 with random change in load	56
Figure 5.30 System frequency response for area 2 with random change in load	56
Figure 5.31 System frequency response after delay of 0.2 seconds with random change in wind speed	57
Figure 5.32 System frequency response after delay of 0.3 seconds with random change in wind speed	58
Figure 5.33 System frequency response incorporating delay of 0.2 seconds with step wind speed	58
Figure 5.34 System frequency response incorporating delay of 0.3 seconds with step wind speed	59
Figure 5.35 Frequency response with delay of 0.2 seconds with random change in load	59
Figure 5.36 Frequency response with delay of 0.3 seconds with random change in	60

load

Figure 5.37 System frequency response at 70 % V2G penetration with random change in wind speed 60

Figure 5.38 System frequency response at 50 % V2G penetration with random change in wind speed 61

Figure 5.39 System frequency response with 50 % V2G penetration with step wind speed 61

Figure 5.40 System frequency response at 70 % V2G penetration with step wind speed 62

Figure 5.41 System frequency response at 50 % V2G penetration with random change in load 62

Figure 5.42 System frequency response at 70 % V2G penetration with random change in load 63

LIST OF TABLES

Table 2.1 V2G model parameters	22
Table 2.2 Capacity of hybrid power system	22
Table 2.3 Capacity of wind system	23
Table 5.1 Random wind speed for step change in load	63
Table 5.2 Step wind speed for step change in load	63
Table 5.3 Step wind speed for random change in load	64

LIST OF ABBREVIATIONS

ACE	Area control error
AGC	Automatic generation control
EV	Electric vehicle
G2V	Grid to vehicle
IAE	Integral absolute error
IEEE	Institute of Electrical and Electronics Engineers
ISE	Integral square error
ISO	Independent system operator
ISTAE	Integral square time absolute error
ISTE	Integral square time absolute error
LFC	Load frequency control
LMI	Linear matrix inequality
PHEV	Plug in hybrid vehicle
PI	Proportional integral
PID	Proportional integral derivative
PSO	Particle Swarm Optimization
PSO	Particle swarm optimization
SCADA	Supervisory control and data acquisition
SOC	State of charge
V2G	Vehicle to grid

CHAPTER 1

INTRODUCTION

1.1 Overview

In later years of this century load frequency control (LFC) is playing pivotal role in designing as well as operational techniques of our contemporary electric power system. According to scenario been presented for recent years, requirement of power has been increased, thus deregulation of power market was required to accommodate rising power demands for consumers. Now when renewable energy is being integrated with regular (conventional) system, it requires to be paramount responsibility for interconnected system is to sustain the frequency within the designated value [1]. The sources of renewable energy can be wind energy, fuel cells, and batteries. The term hybrid or interconnected power system is a system that is connected with contemporary electric system to maintain power supply continuity and quality power is being supplied to consumer end. The era of electric plugged vehicles is expanding because of now contribution of plugged in vehicles (hybrid) in electric power system has been increased due to fast damping result of plugged in vehicles than thermal plant response [2]. Also plug in hybrid vehicles providing auxiliary spinning reserve. Due to continuous variations in wind power and the load, consequence is the frequency disruption of system. Therefore, difference in power between generation and demand needs to be balanced for operation of power system. In an affiliated power system, hybridized escorted by renewable energy, controllers must take care of any disturbances in system. A power system pronounced to be healthy if inclined enough to supply the desired power with condition of maintaining the frequency within acceptable target. The load frequency control loop has to control real power and frequency range. For a considerable size power system with integrated wind power and plugged vehicle energy only load frequency control is important for its operational features [3]. Therefore, smart grid has enabled the new vision for centralized system to become more secure and reliable by incorporating intuitive and intelligent controller to control variations in frequency and tie-line power. When frequency perturbations turn out to be larger, they became rationale for heavy loading of transmission lines, brutalized performance of all equipment's and disgrace

performance of load elements. For interconnected system, it becomes extremely important to have frequency perturbations within acceptable bound [4].

1.2 Literature Review

As resources of renewable energy likely wind, plugged in electric vehicles are there and indispensable and their dummies are non-identical from the governor connected turbine loop, their soundness and dependability being engrossing. For interconnected system, mainly the security and the reliability of system getting to be major review attributable to the multiplying entanglement of power system designing and its operation [5]. Smart grid perception has deregulated the conventional grid more rooted and staunch due to the cultivate technology. The engrossment in plugged in vehicles being proliferated ascribed to their potential to minimize the filthiness caused by carbon dioxide [6]. Today proliferating wind power incorporation into the electric power grid, thus benchmark in terms of frequency perturbation desperate to think over to corroborate system stability and authenticity. So, regulations in frequencies have more deprecatory with the involvement of frequency vulnerable loads with wind in interconnected system. There are much more improvements in the controller designing for LFC, some of them proved to be best than traditional controlling techniques or we can say manual or time consuming [7]. Few of them have been enlighten in literature review section.

During foregone years, the operation of power system has been optimized by various controlling techniques. But moving on to power demand by customers, orthodox system for power system was deregulated. In this way, orthodox system was customized by integrating all possible renewable energy sources. Escalating convolutedness in supervising the immensity in power grid, growing pertain to nature, autonomy for energy sustainability, demand in growth and service quality continuity to accentuate the need for requisition of such kind of automations. Smarter kind of grid is envisioned to take precedence with at one's disposal in contemporary advancement in transfigure the conventional to one that gives us justification more insightful and efficiently [8].

Fortune work will be observant on the amalgamation of all governable load and systematize the optimal potency of hybrid renewable energy. The operation with wind

farm and vehicle to grid with PSO-PI techniques has been implemented in, a control competence is proposed for LFC including wind power for multi area system [9].

The response clarifies the benefits of economic demand and approach that was applied was stochastic. The analysis done on single area power system to show response from demand created in system with power sharing by primary control to check impact in stability of system. The control system framework for power system was then proposed as decentralized one with the help of more than one agent that is spinning reserves like wind, solar added. Now with the practical implementation of reserves of wind and solar, there require compensation for reactive that was main issue in supplying quality of power to other end without any change in verified frequency by controllers [10]. In the same year, the power system controller has adopted artificial intelligence techniques. The response from large wind farms with variable speed wind turbines were modified with primary control of PI and in the secondary control with fuzzy logic control. Then system simulations were performed on IEEE 30 bus system [11]. After PI controllers, then comes part of PID controllers successfully adopted for large wind integrated farms. The LFC loop was coordinated with large wind farms with batteries (Redox flow batteries) [12]. After PI, PID and other control methods, a distributed model approach with predictive control was implemented in system integrated with wind, hydro, and thermal plants for four area control system [13]. Then second order approach with sliding mode were imposed and response was obtained with lyapunov property and robust control system was implemented in [14].

The introduction of smart grid and its implementation started about twenty years ago, as per survey done. Considering most crucial last 6-7 years of research, it has been found that introduction of electric vehicles boosted our normal power with unceasing and worth power supply. Finding electric vehicles, the option for quality and unceasing power supply, we found explication for environmental menace of depletion of exhaustible resources [15]. The battery usage for electric vehicles has made us to think about storage of power generated from vehicles. Earlier fuel cells or ultracapacitors were used. At that time lead acid batteries were also used but, due to their short working life, they were replaced by lithium ion batteries. A new concept appeared in the year 2018, the intelligent transformer that is a transformer that

provides all communication control over smart grid. The proposed paper develops a schematic way of restructuring system from harmonics under variable kind of frequency breach [16]. When large collections of stable or secure systems are integrated with each other than the resulting system will be unsecure one. Paper represents the integration of less stable grids whose controlling can be done with assist of IEEE-13 test feeder given in [17]. For frequency breach, a control method was implementing as double sliding methodology. This procedure was executed on microgrid with PV-Diesel-Wind integration as compensating source in [18]. The concept of stochastic hold algorithm for system to be adapted under frequency variations for active power demand response was presented in [19] with the modules of smarter grid applications in electric world. For an economic operation, a module was designed as multi-client problems solving algorithm for optimal power. This paper was first to introduce dual kind of architecture [20]. Dynamic control model with four area state predictions such that individual area controller assures stability. Uncertainties of a small range were included in distribution system presenting frequency, and tie-line powers of every participating area [21]. A recent paper has designed a real time management and proper control technique for infrastructure like buildings with automated and intelligent control that can only be applicable to hybridized grids (AC/DC) with adequate demand control [22]. Algorithm for controllers were proposed, 3 steps for algorithm were like, the first one for higher point that was included for optimization of conventional plant and wind, the second one for plugged in vehicles and last one for feedback electricity from the grid side. This kind of algorithm with its numerical solutions gave best results for regulation in frequency and other constraints presented in [23]. After the stochastic approaches, probabilistic approaches were adopted, but they were proven inappropriate. Particle swarm optimization (PSO) with evolutionary methods was advocated for integration of PHEV with grid [24]. The optimization problem with different objectives was formulated by PSO with the control over power (active, reactive) of the proposed system. The above mentioned obtained power were tested over IEEE-14 bus system. Their main aim was to control frequency and voltage [25]. The proposed scheme in [26] was developed to bring together the charging power, discharging power of electric vehicles with sources of renewable energy. A new term urgency index was introduced in this paper to verify applications practicality of features like robustness, reliability etc. The frequency perturbation of grid was controlled by movable

batteries. Later on, IEEE 39 bus system was included for charging stations like electric vehicles. The proposed controller had made compared with fuzzy and PI optimized controllers [27].

Now coming towards to the third important work of thesis exertion regarding communication delay in power system. Now a day's, as entanglement of interconnected systems is increased giving way to delaying signals to reach transmitting units and other interconnected communication web. In any case if communication mesh has stopped working due to delay in signals it will ultimately cause changing frequency and voltage fluctuation problem. Communication delay obstacle has been underlined from the beginning of smart grid system. MDP model was introduced in [28], giving ideas about approximations that has been included in paper with effects showing of frequency response. Reference [29] gives idea about techniques used to tackle frequency and other effective issue. Even a delay of few microseconds to seconds can hamper the stability of system. Thus, in proposed paper, the controllers were developed according to analysis of stability and effective operational view. Zhao et al. performed case studies in the system by adopting algorithm to measure stability and robustness and creating contradiction so that mismatch occurs between generation and load provided in [30]. Due to the introduction of smart grid environment, communication network was mostly affected due to loss of information as packet mislaying or failure in buses connected. The paper [31] analyzed degradation of network because of communication failure in system, basic controller design and topologies were main focus for authors for frequency control.

The modern electric power system i.e. smart grid is vulnerable to more threats as attackers can make system to loss packets of information. So, programming was involved to get stable responses from preventing signal mismatch were provided with Markovian attack-defend approach in [32]. In the year 2016, many researches were implemented over topology related to communication delay in the interconnected system network. The effects with time delay, quantization error, information loss in packets were calculated with simulation results in smart grid environment. For this controller was developed using LMI technique was implemented in the [33]. In the year 2017, load frequency control (LFC) was investigated with new term of service

attackers, event trigger communication delay was analyzed in multi area system integrated with the implementation of H-infinity controller. The effectiveness was proved in the case studies of [34]. Predicted LFC and NPLFC approaches were used to find stability and for this, lyapunov theorem predicted robustness of system with communication delays in the interconnected systems [35]. For hierarchical power system when first and secondary predominance failed to supervise the system frequency, then secondary controller is being implemented. Based on the ace power solutions, tertiary power control has to be there for preventing communication information delay [36]. After implementing stability criteria with lyapunov methods, now new way was discovered to find stability with linear inequalities by lyapunov-krasovski theorem. As PI-LFC schematic way was used as controller before. In this paper series of linear inequalities were imposed as delay in system. Some new inequalities imposed are discussed in [37]. In the year 2018, fuzzy-PI controller was implemented on IEEE-39 bus system with minimizing effects of frequency overshoots when communication time delay was included in the system a related scheme of demand response was proposed in [38]. With the advancement in the present year, low order error is compared with elevated order error. In this way cost curtailment is more by implanting the methods of robustness for system which can hold delay of even 20 seconds. This kind of work has been performed in [39], by ensuring even less unfold to consumers utility power.

1.3 Gaps Identified

From the survey part, some points here became gaps in study. Substantial power arrangement in need of non-exhaustible power that consummate with the aid of power from wind, solar, nuclear, and plugged vehicles. The issues that came across survey is control structure for proposed systems. The control design for any system should come across all possible reasons that may hamper stability of propound system. Also, some portion of information may have lost in transmission due to delay in handling information for system. Gaps which are identified likely are the systems to have controllers with fast responding and robust criteria. Depending on penetrations of non-exhaustible resource energies, the response in system received is different for case studies incorporated. The proposed systems do not have the proper solutions for the integral errors that have to be shown which can give us idea about the stability of

the propounded systems. Only few of the researches had been there with integral absolute errors. Thus, the presented research has more integral errors that have been shown in the research work to compare for the stability of the propounded system, to ensure from which error minimizations the presented system is being more stable and for which error, the system needs more corrections. Thus, two area systems is propounded here with the integration of non-exhaustible resources and penetration of power from plugged vehicles is varied. The stability performance of the system is analyzed with new proposed controllers with conventional controller in this report.

1.4 Motivation

From total population of world, India provides home to 17 % of world's population. According to survey of IEA, the energy consumption in India is still 42 % below the total population in 2050. So, this can make you imagine that how much quality of power is required for our country. Moreover, the main problem lies in transmission and distribution line losses, electricity theft and most important is using electricity without even paying for it.

In the year 2012, India gone through major power blackout then researchers find out actual cause behind it. We need to shift focus from traditional centralized grids to smarter decentralized grids, providing additional power back up in the form of battery, or solar or wind. We need to use bio products like biodiesel. According to national bio-diesel mission, by 2030 India is heading towards 105 kilo barrels of oil equivalent per day with biodiesel. The only point for motivation is to involve renewable energy resources more for producing electricity. "MAKE IN INDIA" program has initiated but it requires commitment of social as well as government support. This program can even provide jobs to many unemployed in our country in terms of their security, maintenance for solar panels and renewable field work. This can be more, if buildings would be participating in supplying power to grid. In all aspects, smarter grid would enhance our power sector in a better way in world of quality power (24× 7).

1.5 Objectives

- a) To design 2 area power system integrated with inexhaustible energy source like wind and plug in electric vehicle that can reimburse the ample power when LFC cannot make it.
- b) To keep frequency, tie-line power and area control error within specified limits by using control techniques mentioned in work plan that is PI controller is tuned according to response.
- c) To add communication delay in system to check frequency, tie-line response.
- d) To make state space analysis of model for checking stability condition.

1.6 Expected Deliverables

The proposed work is to deliver a Simulink model of two area that developed system can handle all worst stability conditions in a system. This proposed exertion has incorporation of plugged in vehicle power and wind power that behaves as compensating part for the two areas. In the literature survey segment, the focused part has been the traditional system power compensation with the help of non-exhaustible sources. With great research over papers, now able to present the research work that possess the compensating nature for traditional system. With continuously of wind speed a control schematic developed to have fewer oscillations in the frequency with the Pi controller. Also, different penetration effects of vehicle power in the developed system has been major focus to actually verify the reimburse nature of non-exhaustible resources.

1.7 Organization of Thesis Work

Chapter 1 constitutes for overview, literature review, motivation for work and objectives to be chosen and its work organization.

Chapter 2 will be giving idea about power system configuration and state space modelling giving stability results.

Chapter 3 will add work of communication delay and its effects in system model.

Chapter 4 providing block diagram of model and results obtained.

Chapter 5 finally providing conclusions achieved and discussing about future work.

1.8 Conclusion

From this chapter, the points that came across during research work globally were being same to have complete control over the stability function in any system. With the inclusion of modernized grids in this needy electric world, every possible solution to make our grid integrated system better for every possible worst power failure situations that Indian power quarter has faced during blackout year of 2012. After these researchers propound has only main issues for frequency control. Thus, presented chapter has only main reasons of failure and control issue. Different control schemes have been accentuated that has proved better than the traditional schemes that were used earlier.

CHAPTER 2

DESIGN AND MODELING OF PROPOSED SYSTEM

2.1 Introduction

In the study of alliance power systems, load frequency control need oversight models for their nailed operation. Thesis work comprised of two area system with the amalgamation of wind power as well as charging power from vehicle to grid for particular requirement of demand. Mainly 3 types of instabilities are checked for secure performance but propound work have focused only at frequency unpredictableness. Frequency vulnerability is the ineptitude of a power mesh to perpetuate frequency within the designated operating limits.

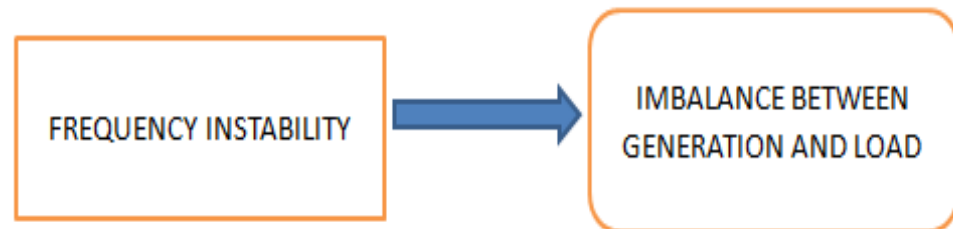


Figure 2.1: Frequency vulnerability

Regulation of frequency in power mesh includes Load frequency control(LFC). When real power is changed, frequency of system is mainly affected. Real power mainly depends on rotor angle and frequency [40]. Main work of lfc is given below

- a. To keep frequency within designated limits.
- b. To control tie line interchange within control areas at arranged values.
- c. Each area of reciprocally connected systems should absorb its own load changes.

As we know that revise in real power only strikes the frequency of power mesh, reactive power is not so much tender to transmute in frequency but mainly contingent on revise in voltage expanse. Load frequency control noose predominate the real power and frequency. Automatic voltage regulator dominates voltage expanse and reactive power while frequency transmute is hanged on transfigure in the defined

rotor angle δ . The aim of this strike is to regulate frequency in interlinked areas and also to tune the power flow over tie-line between the utilities of both the systems.

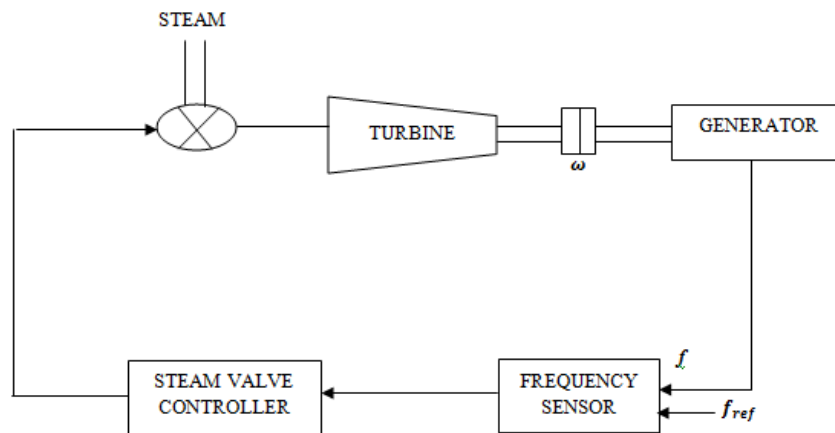


Figure 2.2: Generator with basic frequency control

Power flow over tie lines can be on short term basis or long-term basis if giving and taking the energy in both areas are beneficial to each other. The steam valve has been controlled with the increase or decrease in demand in the system. Rising steam flow means there is demand for the power in the system while falling in the steam flow means the demand for required power has been decelerated. But in the modernized world of smarter power grids there is an issue with thermal plants that their response is slow. Thus necessity with fast power response increases, and this need is accepted by the power that we get from plugged-in vehicles. Vehicles can supply sufficient power when there is scarcity of power. In the future also possible to have homes that involve in the grid power increment. The drop-in frequency should be at bottom over tie line and power flow is amplitude to perpetuate steadiness between generation and load to save profound system from being collapsed [41].

2.2 Modeling of Two Area Power System

The system of two area is proposed with streamline of wind power and electric vehicle power. Thus, variations in the system frequency, area control error, tie line and power capacity of each area is being analyzed. The basic layout of the system shown by the figure below:

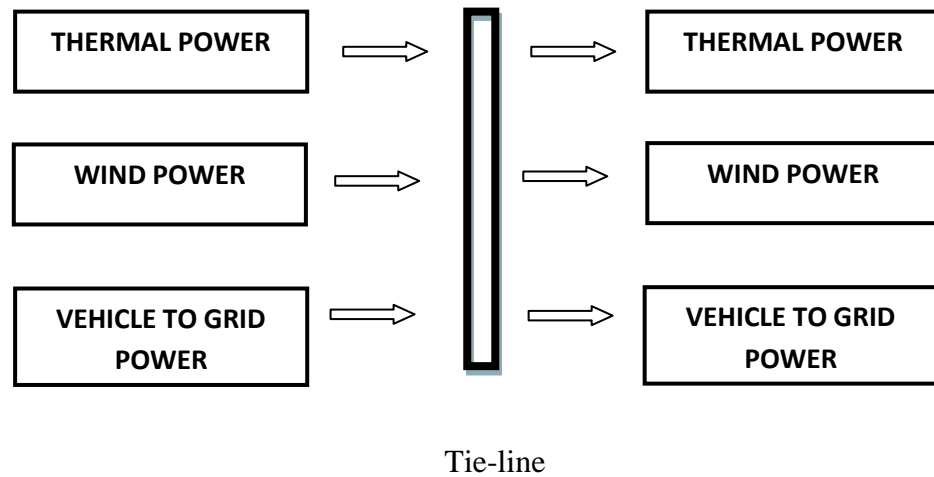


Figure 2.3: Basic layout of system

The LFC problem is comprehensively analyzed as individual areas and multi area by various experimenters with AGC, excitation control design and parametric uncertainty etc. As nonlinearities prevails in modern power system the associated transient may aggravates to wide area which may accompany the blackout schema. Wind integration is mainly the subsidiary retain margin by conventional plants. Modern wind farms running with variable speed wind turbines boosted up the quality of grid power. Thus, drawing together these energy sources shown in above figure, created system for controllable frequency that gives sustain power results.

2.2.1 Linear Thermal Model

The first block that comes for model is thermal part, the second block is LFC block, then after comes V2G block, wind power block and demand block. The block for thermal plant constitute with turbine, generator-load block, power system block shown below. This developed model is linear model with control scheme presented with it in the middle of the model.

a. Turbine Model

The turbine presented here is the non-reheat model whose valve position is decided by turbine output, also it is simple other than reheat and hydraulic turbines. The energy is squeezed from steam and converted into mechanical power ΔP_{Mech} and is further appointed to the generator of the system. The increase or decrease of generation is directly to be contingent on difference in power required.

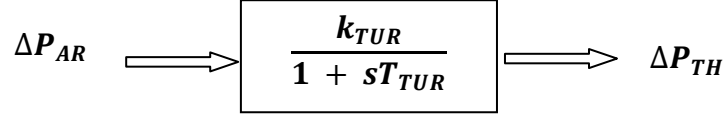


Figure 2.4: Transfer function of turbine model

Here sT_{TUR} being time constant of turbine model and ΔP_{AR} is the required power through LFC controller.

b. Generator - load Model

From the turbine output, the generator transforms the mechanical energy into electrical energy. The task of storing large aggregate of power is difficult, thus requires balance between load demand and generation of power. Thus, it is mandatory to have $\Delta P_D = \Delta P_{TH}$ for stable operation of thermal plant.

The following are some assumptions for proposed system are

- The nominal frequency is F^o and system is in normal position due to power balance.
- The generation is directly dependent on demand required in the system i.e. $\Delta P_D = \Delta P_{TH}$.
- The power absorbed in the system is dependent on two things i.e. kinetic energy of generator rotor and load on motor depends directly on speed of turbine.

The kinetic energy is represented by W_{KIN} as kinetic energy is directly proportional to square of speed of the generator given by the equation below

$$W_{KIN} = W_{KIN}^o \left(\frac{F}{F^o} \right)^2 \quad (2.1)$$

Where F is the change in frequency according to load and $F = F^o + \Delta F$

As the rate of change of load with respect to the frequency is constant, this is given by the equation is

$$G = \frac{\partial P_D}{\partial F} \quad (2.2)$$

For the net power equation

$$\Delta P_{TH} = \Delta P_D + \frac{d(W_{KIN})}{dt} + G\Delta F \quad (2.3)$$

Now neglect the term ΔF and higher order terms the equation for kinetic energy becomes

$$W_{KIN} = W_{KIN}^o \mathbf{1} + 2 \frac{\Delta F}{F^o} \quad (2.4)$$

Power equation becomes

$$\Delta P_{TH} = 2 \frac{W_{KIN}}{F^o} \frac{d(\Delta F)}{dt} + G \Delta F + \Delta P_D \quad (2.5)$$

Now at particular frequency, the kinetic energy stored is given by

$$W_{KIN}^o = H \times P_R \quad (2.6)$$

Where H is the inertia constant and P_R being rating of power

After dividing equation 2.5 by P_R the new equation is

$$\Delta P_{TH} - \Delta P_D = 2 \frac{H}{F^o} \frac{d(\Delta F)}{dt} + G \Delta F \quad (2.7)$$

Above equation can be written as

$$\Delta P_{TH} - \Delta P_D = 2H \frac{d}{dt} \left(\frac{\Delta F}{F^o} \right) + G F^o \frac{\Delta F}{F^o} \quad (2.8)$$

With Laplace transform of equation 2.7 it is written as

$$\Delta P_{TH}(s) - \Delta P_D(s) = 2 \frac{H}{F^o} s \Delta F(s) + G \Delta F(s) \quad (2.9)$$

Now final equation becomes

$$\Delta F(s) = P_P(s) [\Delta P_{TH}(s) - \Delta P_D(s)] \quad (2.10)$$

$$\text{Where } P_P(s) = \frac{K_{PS}}{1 + sT_{PS}} \quad (2.11)$$

$$T_{PS} = \frac{2H}{F^o G} \quad (2.12)$$

$$K_{PS} = \frac{1}{G} \quad (2.13)$$

The transfer function for generator load model becomes

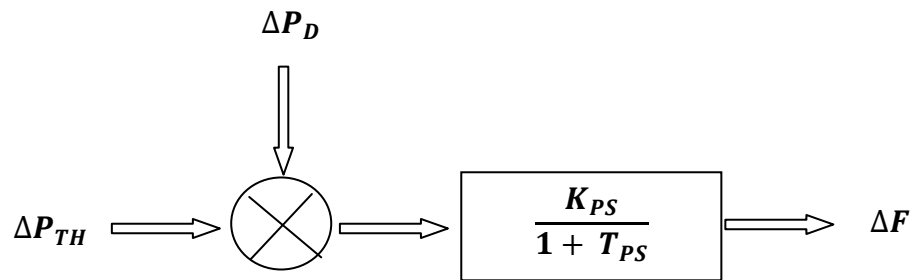


Figure 2.5: Transfer function of Generator- Load model

Here ΔP_{TH} is the required thermal power and ΔP_D is the disturbance in the form of wind power or may be vehicle power.

c. Governor Model

The governor controls the flow of real power in the proposed system. The generator output is balanced by the turbine output. Speed limiter is also another name for governor. No doubt about governor controls the speed, power in turbine and also frequency of the hybrid system. The valve position that is opening and closing of valve is maintained by only governor. The governor system provides a control mechanism to have frequency within prescribed limits. The transfer function model of governor is given below.

$$\Delta P_G = \Delta P_{AR} - \frac{1}{R} \Delta F \quad (2.14)$$

$$\Delta P_V = \frac{\Delta P_G}{1 + sT_G} \quad (2.15)$$

Here T_G is time constant of governor model and ΔP_V is the power from generator part of thermal system.

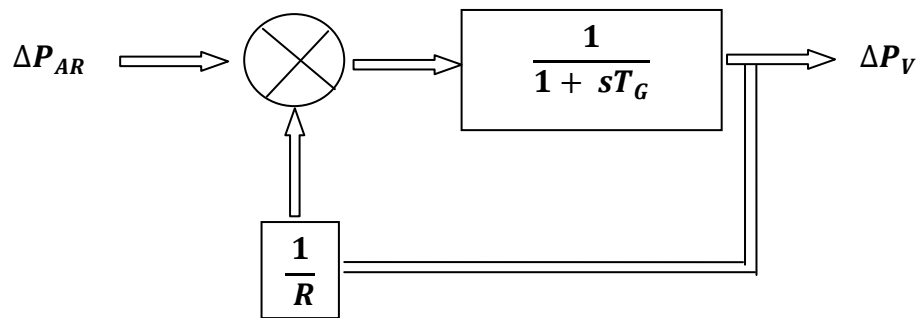


Figure 2.6: Transfer Function of Governor model

2.2.2 Linear LFC Model

The output of this model is being given to change in load parameter. The block before PI controller work as delay. Thermal plant gets input power from LFC model shown here below. In the traditional system the response was sluggish because primary control of power was not fulfilled, and then moved for secondary control with proposed control stratagem. This control stratagem has given better response than only with PI controller. The LFC individually cannot reimburse all the controlling function for the propound system, this requires another secondary control to have a better response than alone with PI controller. The reason behind involvement of

another control work to have a response that mitigated the main problem in all smarter power systems.

Mathematical model of LFC is given below

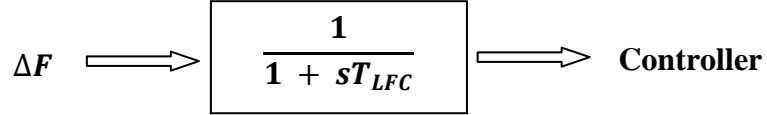


Figure 2.7: Transfer function of LFC model

Here sT_{LFC} is the time constant for LFC controller.

2.2.3 Linear Vehicle Model

The output from LFC will be provided to thermal plant for convenient operation of hybrid system. Whereas the abbreviations for T_{LFC} work as a filter circuits for system or say functions as delay.

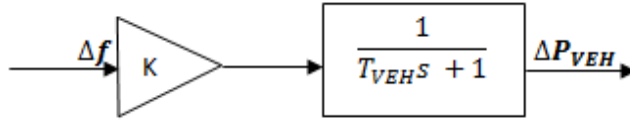


Figure 2.8: Transfer function of vehicle model

The input for the above model is from LFC model and its output will be given for load change parameter. The term T_{VEH} is the filter circuit being given for the linear function. The supply of power and demand for load disproportion from the interconnected grid can be distinguished from the frequency perturbation. Therefore, V2G power ΔP_{V2G} is made to reign with peculiarity against the frequency perturbation Δf .

Using equation

$$\Delta P_{V2G} = \begin{cases} K_{Vehicle} \Delta f & (|K_{Vehicle} \Delta f| \leq P_{max}) \\ P_{max} & (P_{max} < |K_{Vehicle} \Delta f|) \end{cases} \quad (2.16)$$

The term K in figure is represented as $K_{Vehicle}$ is the gain for proposed PHEV tuned by taking output of the V2G effect and the SOC perturbation bounds into considerations.

P_{max} will be the maximum V2G power. If the frequency perturbation plunge below a minimum least value, then paramount discharge is instant allocated for the grid.

$K_{Vehicle}$ will now be calculated from the equation given below

$$K_{Vehicle} = K_{max} \left[1 - \left(\frac{SOC - SOC_{(high)}}{SOC_{(min)} - SOC_{(high)}} \right)^h \right] \quad (2.17)$$

Here terms SOC_{min} , SOC_{high} , and h are the base SOC, low SOC, high SOC, maximum SOC, and designing specifications severally. The gain can be obtained from following linear equations that has been developed. These are the design parameters used as a transfer function for finding vehicle power.

The SOC (STATE of CHARGE) is explained as ratio of capacity of a battery which is remaining the full charged capacity. Acc to this definition explained above a fully charged device has an SOC of 100% and a fully discharged device has an SOC of 0%. In proposed linear vehicle model the term K is the $K_{Vehicle}$ that will be calculated for vehicle to grid power penetration in the model and results according to which are presented in chapter 5. The vehicle to grid power penetration hinged on the aggregate of power required for the system, because the control of LFC will have less influence in the system that is why non-exhaustible energy source has been used to reimburse the exiguous power in two area system. The outputs that got after proper simulation of these makes to conclude that wind and other non-exhaustible source can exactly make over the deficient power for the required system. This propound two area system has been shown in next page with the block diagram covering all blocks for the propound model.

2.2.4 Wind Power Model

As wind speed is continuously varying and wind power is dependent on wind speed. Fixed speed variable turbines are directly connected to grid possible with control over active and reactive power and reduces almost stress of mechanical parts employed. The aerodynamic model of wind provides effect of coupling between mechanical torque and speed of wind. The pitch controller acts when there is any problem in shut down or startup of wind turbines. The pitch controller regulates the wind power. At lower speed of wind pitch angle is lay down to zero degree and pitch angle increased

when wind speed is higher for releasing the excessive power (mechanical) restricting speed of rotor. In simulation pitch angle is set at 0 degree at lower wind speeds for representing the optimum pitch angle. Now the wind turbine power is given by

$$P_{WIND(pu)} = \frac{(\text{Step Load (pu)} \times \text{Wind Turbine Power (MW)})}{\text{Total Load (MW)}} \quad (2.18)$$

Here $P_{WIND(pu)}$ is the total wind power in per unit, step load for area 1 is 0.01 per unit and for area 2 is 0.002 per unit. Their numerical values are given in table section of wind turbine parameters.

The transfer function for wind turbine is given as

$$G_{WIND} = \frac{K_{WIND}}{1+sT_{WIND}} \quad (2.19)$$

Where T_{WIND} is the time constant for the wind system

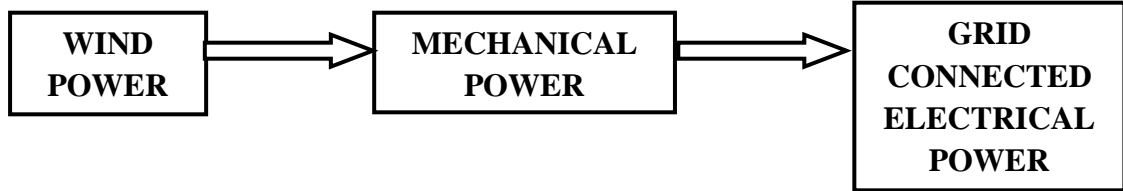


Figure 2.9: wind power block diagram

The basic idea behind wind power supporting electrical power is that the wind power is converted into mechanical power through aerodynamic torque. The wind energy converted into mechanical energy by wind turbines having more blades. Wind energy system is connected mechanically through electrical system. This mechanical power runs the turbine of the electrical system and mechanical energy of shaft is converted into electrical energy. Few of the pros of the fixed speed wind turbines are low cost, free of maintenance, no brushes are required and construction is rugged. The listed price of fixed speed wind turbines is much less than variable speed wind turbines. This is because of the rotor whose speed is constant and has more load than variable operation. This reduces the costing of fixed wind speed system and for this squirrel cage induction generator is pre-owned. Because of large speed difference between induction generator (squirrel cage) and the turbine hub, a gear box is used. The squirrel cage induction generator works on principle of consuming reactive power. The reactive power is supplied from the interconnected network to the stator winding for developing rotating magnetic field in the induction generator. But for weaker grids

and larger turbines it becomes undesirable to have good power factor. Thus, for reactive power a compensation capacitor banks are required for making steady state power factor to one.

2.2.5 Two Area Power System Interconnected by Tie Line

Tie line is the only medium of transferring powers from system 1 to 2 and its vice-versa. Regulation of frequency and flow of power is the only target of tie line. Tie line power flow can be short or everlasting if there is mutual consent of transfer of scheduled energy between the interconnected systems. Both the areas will compensate power if there is shortcoming of power in either of the interconnected systems. The mathematical expression for tie line power is

$$P_{12}^{\circ} = \frac{|V_1^{\circ}| |V_2^{\circ}|}{X} \text{Sin} (\delta_1^{\circ} - \delta_2^{\circ}) \quad (2.20)$$

Here X is tie line reactance

P_{12}° is power transmission from system 1 to 2 and $\delta_1^{\circ}, \delta_2^{\circ}$ are phase angles for voltages V_1°, V_2° respectively.

Considering small deviations of angles $\delta_1^{\circ}, \delta_2^{\circ}$ let power transfer is defined as ΔP_{12} is given as

$$\Delta P_{12}^{\circ} = \Delta T (\Delta \delta_1 - \Delta \delta_2) \quad (2.21)$$

$$\text{Here } T \text{ is synchronizing coefficient} = \frac{|V_1^{\circ}| |V_2^{\circ}|}{X} \text{Cos} (\delta_1^{\circ} - \delta_2^{\circ}) \quad (2.22)$$

Change in frequency deviation is given by the equation

$$\Delta F = \frac{1}{2\pi} \frac{d}{dt} (\delta^{\circ} + \Delta \delta) \quad (2.23)$$

Equation 2.23 can be written as

$$\Delta F = \frac{1}{2\pi} \frac{d}{dt} (\Delta \delta) \quad (2.24)$$

$$\Delta \delta = 2\pi \int \Delta F dt \quad (2.25)$$

Now taking Laplace transform of equation 2.21 is re written as

$$\Delta P_{12}^{\circ} (s) = \frac{2\pi T_{12}}{s} [\Delta F_1(s) - \Delta F_2(s)] \quad (2.26)$$

2.2.6 Area Control Error

Area control error is the signal in which all tie line power is aided to bias error. This ACE is related to speed changers of every generators of thermal plant. The area control error is proportional to the exact total exchange in powers of the

interconnected system. The area control error is expressed in terms of bias error and frequency in combination with total power in exchange within system. The equation for tie line is given as

$$ACE_j = \sum_i^K \Delta P_{ji} + \alpha_j \Delta F_j \quad (2.27)$$

2.2.7 Power System Model

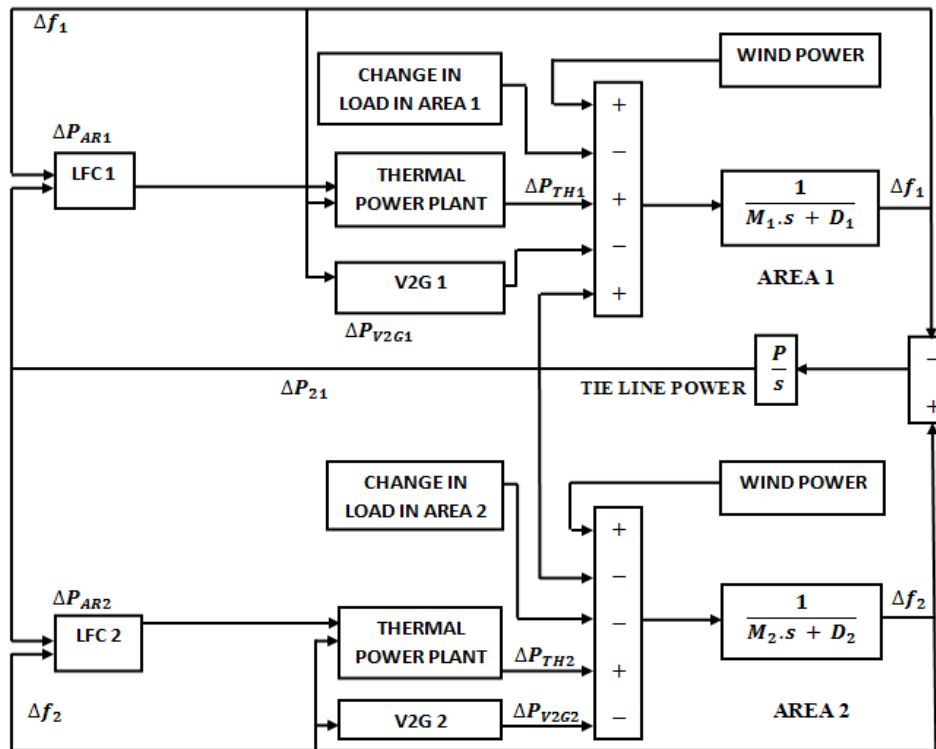


Figure 2.10: Proposed power system model

This propound model is thrived for furtherance of derivative model that were been into practice few decades but due to increasing scarcity in power claim with retaining worth of power. It became need of this decade.

The working model is emanating in per unit system. It is imperative to disclose that LFC auditor not have potential to encounter power, so in order to come across demands of lager system there require non-exhaustible source like electric vehicles plugged in utility and wind power. Thus, got response with minimum perturbations in frequency, area control error, and tie- power for propound two area system.

According to the survey in previous chapter, thermal plant feedback is slower so faster response with plugged vehicles will reimburse the deficient power and wind power that is always being in fluctuating nature. As per survey of wind plant, we get to know that during night hours' time, speed of wind is more than during day time, wind plants are more in working at night and that fluctuating speed of wind will need a controller that will be discussed further in the next sections.

Nomenclature for propound model

Δf_1 =Change in frequency for area 1.

Δf_2 =Change in frequency for area 2.

ΔP_{V2G1} =Change in power from vehicles for area 1.

ΔP_{V2G2} =Change in power from vehicles for area 2.

ΔP_{TH1} =Change in power from thermal plant for area 1.

ΔP_{TH2} =Change in power from thermal plant for area 2.

ΔP_{12} = Change in tie-line power.

M_1 = Inertia constant for area 1.

M_2 = Inertia constant for area 2.

D_1 = Load damping constant for area 1.

D_2 = Load damping constant for area 2.

Table 2.1: V2G Model Parameters

PARAMETERS	AREA 1	AREA 2
Maximal Vehicle Power (P_{max}) KW	5	5
Maximal Vehicle Gain (S_{max}) KW/Hz	200	200
$h, SOC_{min}, SOC_{low}, SOC_{high}, SOC_{max}$ %	2,10,20,80,90	2,10,20,80,90
Delay Time (T_{veh}) of Vehicle	1	1
No of PHEVs used	60000	60000

Table 2.2: Capacity of Hybrid Power System

PARAMETERS	AREA 1	AREA 2
Load Capacity (MW)	33090	7090
Load Capacity (pu)	0.01	0.002
Inertia Constant (s)	8.58	9.02
Wind Power (MW)	3600	3000
Wind Power (pu)	400	333.33
LFC Capacity (MW)	496	106
Kp, Ki	0.0062	3.2185
Load Damping Constant (puMW/Hz)	2	2
Grid Constant (puMW/puHz)	8	8
Tie Line Power Coefficient (s)	14	14

Table 2.3: Capacity of Wind Plant

PARAMETERS	VALUES
Rated Power (MW)	9 MW
V _{ph} (V)	575
No of Poles	3
Pitch Angle (deg)	0
Grid Frequency (Hz)	60
Maximum Pitch Angle (deg)	45
Stator Resistance (pu)	0.004843
Stator Inductance (pu)	0.1248
Rotor Resistance (pu)	0.004377
Rotor Inductance (pu)	0.1791
Magnetizing Inductance (pu)	6.77
Inertia Constant (H)	5.04
Friction Factor (F)	0.01
Base Wind Speed (m/s)	11
Pitch Angle Controller Gain k _p ,k _i	5, 45

2.3Conclusion

This chapter is all about how two area interlinked power system has been modeled. All the sub parts of the proposed model have been described in above mentioned sections. The per unit wind power has been provided to both areas and vehicle model power has been calculated depended on the penetrations adopted. The thermal plant

has sub parts of governor, turbine and generator-load models each of them having different role in the proposed system. As thermal plant and LFC controller was incompetent to give right amount of required power in system to have frequency within limited desirability. The frequency has been regulated with the incorporated non-exhaustible resources. The proposed two area power system has desirable results related to frequency, area control error, tie line power and others too.

CHAPTER 3

PROPOSED CONTROLLER FOR TWO AREA SYSTEM

3.1 Introduction

For proposing a power system, it requires a system model, analysis of that model and controlling of that proposed model. In a power system frequency is intimately concerned with electrical speed of the synchronous generators. Further difference between electrical and mechanical torques supervise the rotor acceleration of generators in power system and these are balanced if mechanical and electrical power are continually matched to maintain constant speed. There is need of controller which assists these functions. As frequency breach of + 2 Hz to - 2.5 Hz is not acceptable for more than 60 minutes by steam turbine. Thus, controller is important which can give instant feedback for frequency control. In India acceptable range of frequency is between 49.0 Hz to 50.5 Hz according to power system operation corporation limited. Thus, control action should be robust to give immediate response to the system. The proportional integral controller is used where is no issue of speed of response. This controller finds its applications in industries considering its low cost, non-complex structure and easy to design. In this chapter of controller, the working and explanation of PI controller and proposed controller that multiple uncertainty control is provided. The enhancement of proposed controller over conventional controller (PI) is being notified with better response. The proposed controller has an edge over results perpetuated from conventional controller and thus marks better controlling option over the previous one.

3.2 Design of Controller for Proposed Two Area Power System

The working of power is incomplete without the incorporation of controller. The least stability of any system is only because of indigent performance. As we are familiar that proportional control is predominant control. The predominant control is the most immediate control of power system. With the reference values constant, primary control is the exertion of governor because of change in system frequency. But the limitation causes sluggish feedback. The system might get overload if there is no uniform gain of the system. Also, the primary control has slender control conserve.

Thus, primary control may not retain nominal frequency (60 or 50 Hz) alone by governor action. But the action of primary control is faster than secondary control. Also, in primary control action all the system takes active participation in frequency reimbursement, but for secondary control the unbalance system has to take part in restoration of frequency. There requires secondary action for this. Basic meaning of secondary control is sharing of load by generation group. What secondary control is following the primary control with the cause of increasing power leads to rehabilitation of frequency in any system. Tertiary control only depends on the aim of power system and which role is played by power system in maintaining all its designated features. The secondary control is important in power system because it eventually reduce the error (Integral Time), releasing the control reserves of primary action.

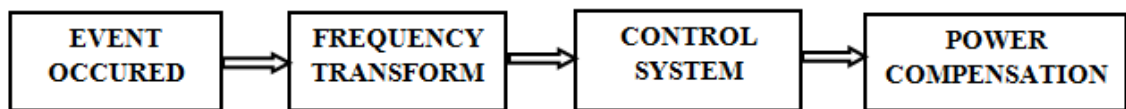


Figure 3.1: Basic controller

Thus, we can say that the range of secondary control action lies in the range for adjustment of power of secondary control action and the action of secondary control is that affirmative part that range lies in between the maximum attained value and the working value.

3.2.1 Conventional Controller

Whenever the integration of wind plant is with traditional power system, this change makes our system necessitate for controllers. In the literature survey, I already mentioned about variegated controllers that has been used to control perturbations in frequency, area control error. Controller which had used in my model is proportional integral. The controller is modulated for different values of K_p and K_i . Then finally repossess that values which proved to be superlative for propound system. The controller is placed before thermal plant for controlling standard deviations in the system [40].

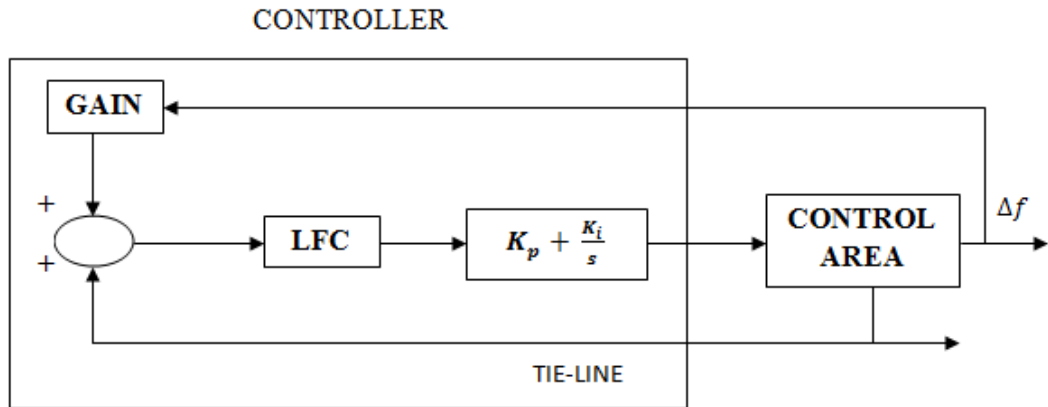


Figure 3.2: Proposed PI controller

This controller was not new for my work, but it requires control advance towards model. This requires approach towards minimum error fluctuations. The used controller will abbreviate the steady state error to zero. As we know that the time constant for closed system is much smaller and if we are going to commute regulation then automatically frequency error will reduce. Using integral controller, speed can be recovered to supposed value. Only PI controller cannot do the controlling thing alone it requires some advance control scheme to get fine kind of results. For that a control pattern is developed that will reduce error conditions to its minimum. Without this scheme, our controller was insufficient to get maximum exact and appropriate results. So, explanation of controller is must to give ideas here about its working. In PI controller, the integral part has work for system to return to normal stage after disturbance occurred [41]. The PI controller can only be used when having large transport delays in the system, no fast response is required for the system, used only if one storage process is being used either inductive or capacitive. PI controller employed in the system if there is presence of large proportion of noise and disturbance in the system. But PI controller despite of such good back there are some disadvantages like increase in overshoot and settling time, some change in steady state error, and stability is not up to the worth point in proposed system. Also, the response of propound system with PI controller has large frequency breach. Thus, required to have new robust control that can compensate the stability of the proposed system. The tuning of controller would be incomplete with the developed scheme for smooth working of controller that will be explained in next section.

3.2.2 Design of Multiple Uncertainty Based H–Infinity Controller

It is foremost to know about H-infinity controller and working. A robust control technique of control theory dealing with improbabilities in its approach for any controller designing, this is defined as H-infinity controller. The control method for robust technique works until the subjected turbulences are within prescribed limits. The H-infinity controller loop forming is a planned control methodology. The performance criteria of H-infinity controller are based on bounded differences encountered between the real plant and the nominal plant resulting in a loop shaping methodology. H-infinity is mostly used for multiple input and multiple output systems. It has been verified after getting results this scheme developed has some great effect on the system with the corresponding effect of PI controller. The PI controller used won't be able to reduce those deviations alone that prevailed in the system. The steady state error was not minimized with the conventional controller. Thus, we need to define its working here, had shown in figure about its functions.

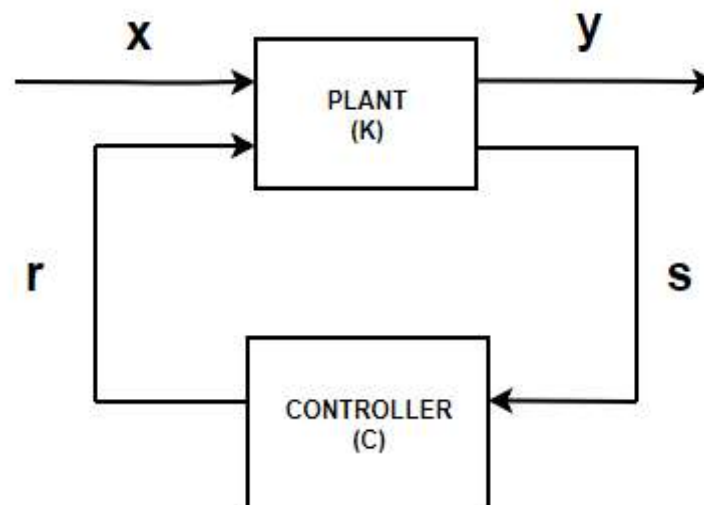


Figure 3.3:Block diagram of H-infinity Controller

Here x is the extrinsic input which includes the disturbance and the reference signal and r is the controller variable. There are two outputs of the above system, one is y which is error signal which is to be minimized and other one is measured variable s that will be used to control the system.

3.2.3 Working of Multiple Uncertainty Based H–Infinity Controller

The optimization criteria for the proposed system is measured in H_∞ norm which is basic of robust control theory treating all objectives of disturbances occurred in the system. The proposed two area system has performed well with H_∞ controller and has better feedback than PI controller. Multiple uncertainty has been incorporated in the system as shown below.

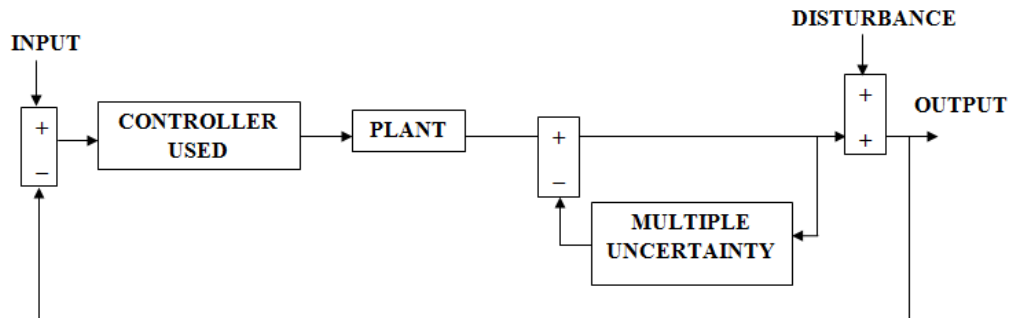


Figure 3.4: Multiple Uncertainty Based H-infinity Controller

This scheme has been imposed in my model to get much accurate results with minimum perturbations and also with continuous and proper tuning of integral and proportional control within the system. The multiple uncertainty includes the integrator function which helps the system to reduce error with each step of simulations. The inverse output is being given here as multiple uncertainty which will sustain proper functioning of controller as well as system response. This multiple uncertainty can be different load situations, variations in parameters of the implemented system. The response from only PI controller are totally non-identical than with proposed multiple uncertainty-based controller. The response with conventional controller was sluggish as compared to multiple uncertainty-based controller. Adding gain with the integrator and tuning with proportional and integral control integrals found to have robust control over conventional system controller. This developed controller will have minimum perturbations and system is a robust one.

Nomenclature for the above system

K is the nominal plant

C is the proportional integral controller

S be the controller input

Δ_{MU} is the multiple uncertainty in the system

\mathbf{r} be the reference input to the nominal plant

\mathbf{y} is the overall output of proposed system

The mathematical modeling of the proposed system with inverse output multiple uncertainty is based on the small gain theorem. For tuning PI controller parameters in LFC for each area of the proposed system, there applied inverse output multiplicative perturbation for modeling the system uncertainties. The control system is shown in above figure 3.4 with nomenclatures for each parameter. The multiple uncertainties are in the form of different loading and generating conditions of thermal plant which is considered here as nominal plant.

According to small gain theorem, any system is stable if

$$\|\Delta_{MU} (\mathbf{J} + \mathbf{CK})^{-1}\|_{\infty} < 1 \quad (3.1)$$

Then the equation is

$$\|\Delta_{MU}\|_{\infty} < \frac{1}{\|(\mathbf{J} + \mathbf{CK})^{-1}\|_{\infty}} \quad (3.2)$$

From equation 3.2, the right side indicating size of the system uncertainties or we can say that stability margin with respect to system uncertainties.

Thus, by minimizing the $\|(\mathbf{J} + \mathbf{CK})^{-1}\|_{\infty}$ the stability margin of the proposed system will be maximum. For designing the robust controller, the equation becomes.

$$\mathbf{G}_{\infty} = \|(\mathbf{J} + \mathbf{CK})^{-1}\|_{\infty} \quad (3.3)$$

Now we will find tracking error $s(t)$

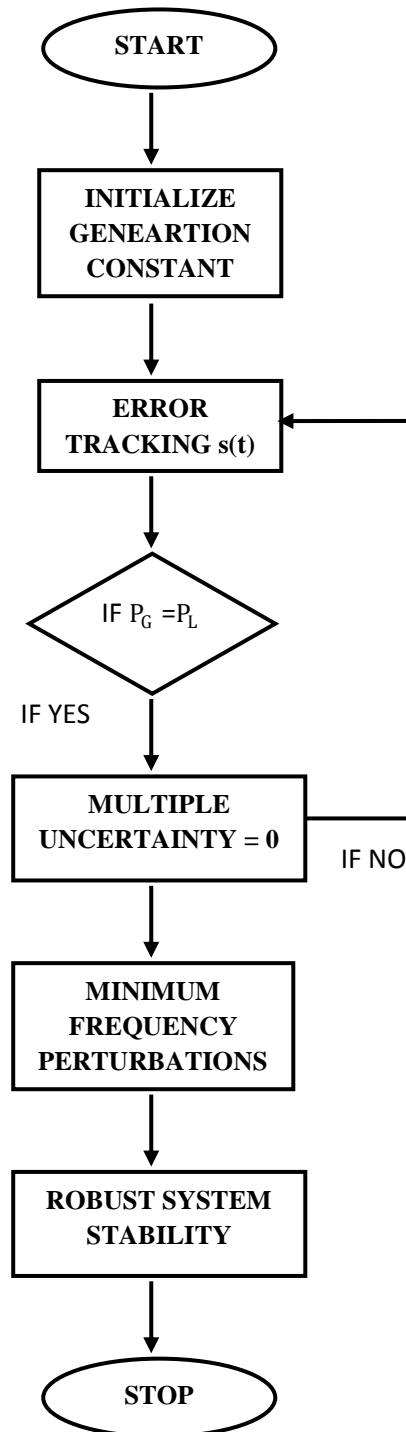
$$\mathbf{s}(t) = \mathbf{x}(t) - \mathbf{y}(t) \quad (3.4)$$

The tracking error is obtained from Laplace transform of $s(t)$ with $\Delta_{MU} = 0$ which is

$$\mathbf{S}(s) = (\mathbf{J} + \mathbf{CK})^{-1} \mathbf{X}(s) \quad (3.5)$$

These equations determine the stability region for the proposed region and error will be minimized for each steps. With each steps of simulation, the error will be minimized till the multiple uncertainties become zero. In other words, we can say that generation and the loading of the generators becomes equal.

Flow chart showing working of H_∞ controller



The above flowchart is showing basic working of proposed controller. This method of control is found to be robust and mean while the deviations in the system has been reduced. This proposed control implemented in the model has the integrator and gain blocks which reduces the error in the system. The integrator block and the gain block continuously minimize the tracking error with each second of simulations. The tracking error is calculated till the generated power and the load demand becomes equal. When both are equal then system stability is achieved. Thus, proposed system stabilized with the multiple uncertainty based H_∞ controller. The proposed controller is robust and its response is better conventional controller response. Also, the integral errors calculated for the proposed model has been reduced with the H_∞ controller.

3.3 Conclusion

The concluding points that come across at the end of this chapter have been mentioned in this sub section part. Just LFC control was unable to have mitigating response of frequency as well as statutory power in the developed system. The two-area smart hybrid power system is developed with the incorporation of plugged in vehicle power, thermal power and wind power. Frequency control, tie line power control is only main focus for this chapter as well as for research purpose. The wind speed being oscillating in nature, thus require controller action need to get leading response after being incorporated in the system. Reimbursement of system power is done by applying wind power with the supplement of plugged in vehicle power. The reason for including vehicle power is, because the thermal plant has slow operational response. The control action of PI controller was improved by the proposed multiple uncertainty-based controller in all respect. Thus, getting minimum perturbations in relations of frequency response, tie line power and at last area control error. Thus, we can say that proposed H_∞ controller based on multiple uncertainties has an edge over conventional PI controller.

CHAPTER 4

MODELING OF TWO AREA POWER SYSTEM WITH COMMUNICATION DELAY

4.1 Introduction

In the literature survey segment, researchers have given some overriding concepts about predominant of delay. Power grids are now a day's constantly streamline by updated technologies to improve efficiency, for monitoring and control with reliability and sustained supply as well as distribution. Due to updating of grids, they are now becoming more and more unfortified because of delay attacks in closed system [42]. The attackers can adopt any method to get their wishes fulfilled by attacking the security shield of system. Present modernized grids have SCADA systems or other intelligent system that provides some kind of relief from being knocked by outsiders. But latest trends to hamper security is to get false information that were being sent to system from a feasible source so that system stability can be alter and system leads to collapse. If no exact measures are adopted then we are going to lose system performance in terms of reliability, stability. There had been several reports from cyber cell about the false information injection. This kind of injections in system has brutally hampered the communication routes in interconnected system and because of such activities valuable information is lost in channels only and receiver at the other side may not get accurate response and stability might be affected. The delay in time to pass information prompt by developed communication mesh will full supremacy of load frequency control (LFC) of system that may or may not include any other microgrids. In transmission of remote computations and other controlling commands, an unlatched communication mesh usually instigates some time delays into LFC loop that ascendance the stability of the alliance system. The microgrids inclusive all conventional power generations, some kind of energy storing devices with distributed generations of power operates having spare flexibility, and the electric vehicles (EVs) that are rooted on automation of vehicle to grid are made to partake in LFC to abridge mission of costs as linked through communication to the grid. Therefore, it is need of hour to research the LFC scheme of grid linked power

system together with communication delay with designing better robust controller for a system to bear all the perturbations [43].

4.2 System Performance with Communication Delay

For my two-area system, with the confederate of wind power and plugged vehicles, get to reimburse my system stability after the instigation of delay in propound system. After the delay introduction then got some deviated results than results before the delay part in propound system. An improved version of infrastructure is required after the instigation of communication slowdown in the system. An Independent System Operator (ISO) always require an improved communication infrastructure because of the monitoring of all network elements under their control. In framework of large utilities, whenever communication lines fail to give response within frame of seconds then messages through telephonic media can also be conveyed in case of communication failure between utilities. This resulting in delaying of secure information exchange within interconnected system. This can be verified in next chapter of results with their justified discussions. Below figure is showing model used for work.

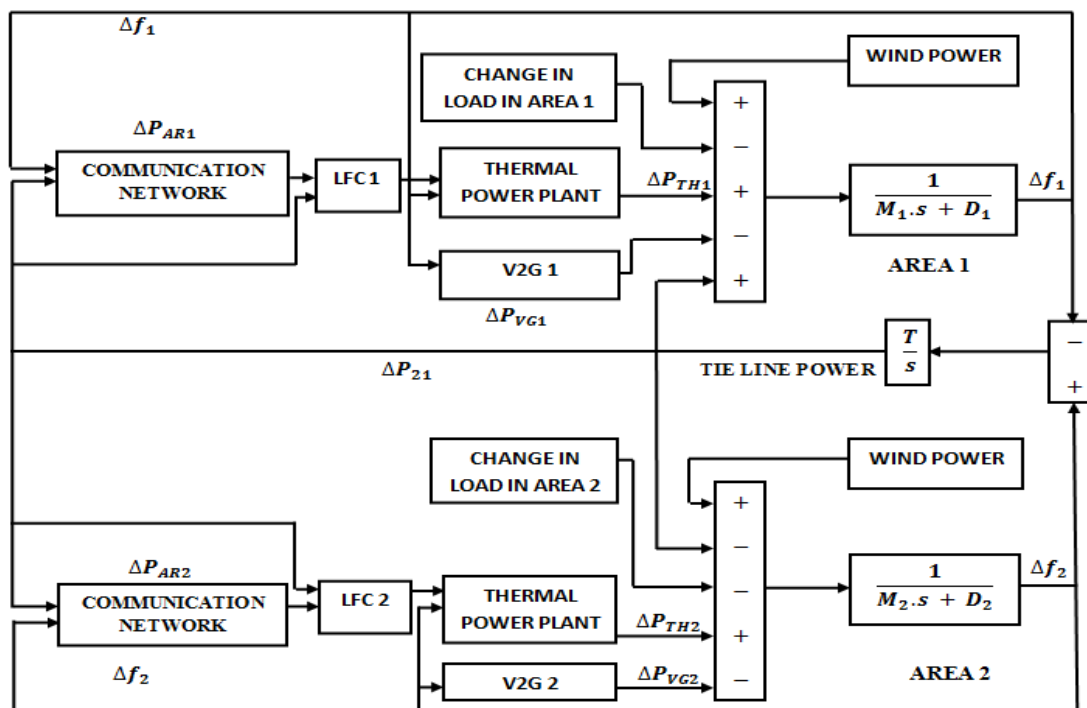


Figure 4.1: System with introduction of communication delay

4.2.1 Incorporating Communication Delay in the System

In the traditional power systems, the communication links in the system have constant time delays throughout system but in smart power system we have variable time delays that need robust controlling scheme for maintaining stability throughout the operation. There is also random nature of delays in closed system. It might get happen that some packets that were sent first may receive later in the system. Throughout the Simulink model, a block of delay has been added to the system when investigating about time delay [44].

Delay block which has been used in simulations has zero pade order. MATLAB provides us Simulink block that enable us to find different pade orders like zero order, first order, second order up to fifth order. In secondary control loop, the delay is contemplated as single instant delay because of the entanglement of closed control mesh. For modeling time delays in continuous time systems, computational and transport delay blocks can be used available in Simulink library. In communicated system, the time delay introduced as area control error signal. The basic meaning of delay means the information takes time to reach the object and controller action does not have time to retain its stable output for previous action of governor. The propound model has application of delay introduced with the help of pade approximation. Time delay of T seconds can have Laplace transform of e^{sT} . In control systems involving closed loops, for imprecise dead bands in system pade approximations are being used as discussed in survey section.

Pade approximations providing us determinate dimensional conjecture of the dead time in system. As we are familiar that dead time in closed loop system are much strenuous to simulate it and explore, so low order delay is comprehending. One reason for closed loop system is that they have infinite numeral of poles so it becomes more and more sophisticated to control such system without robust and rugged controller. The actual megawatt systems have to face large number of parallel hindrances in form of continuous, constant delays affecting the whole power circuit. The motivation behind the incorporation of delay is only to realize that hacking of power flea market e.g. hackers may send false information as signal in the system. Let's have an idea if our governor whose speed is slow gets response from valve to speed up turbine, it might be possible to have false slam on generating utilities. Thus,

need to have control these non-occasional delays in slots of information. The results that got after the introduction of delay part was different than without including the time delay. The results have been presented in following next chapter with their proper discussions.

4.2.2 State Space Analysis

With the two-area system, now consider its state space analysis. Developing as differential equations in which load fluctuations are considered with constant values of wind and vehicle to grid in system. The state space model has input disturbances of wind power, hybrid vehicle power and step or random change in load according to its requirement in the system. But the large disturbance is wind power and vehicle power. The model needs to be evaluated for the state analysis is shown below.

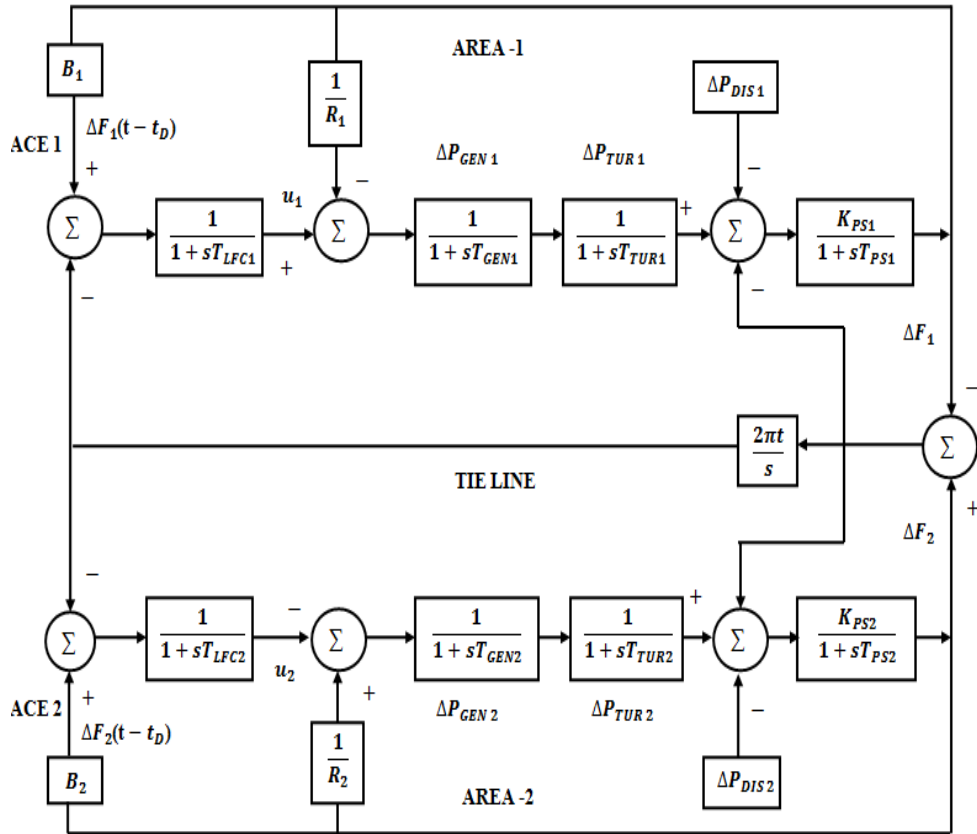


Figure 4.2: State space model of two area interconnected system

Considering all blocks, write differential equations for each block in above figure and tried to get state equations. Where ΔP_{DIS1} , ΔP_{DIS2} are the disturbance inputs, u_1 , u_2 be the control inputs for each area. The disturbance inputs are wind power and vehicle

power and their constant values are included in the per unit system. The rest of the variables in each block like $T_{LFC}, T_{GEN}, T_{TUR}$ and T_{PS} stands for generator, turbine and power system and LFC behave as area control error. These are state variables for each block in both the areas.

For power system block in area 1

$$\Delta F_1^\circ = -\frac{1}{T_{PS}} \Delta F_1 + \frac{K_{PS1}}{T_{PS}} \Delta P_{TUR1} - \frac{K_{PS1}}{T_{PS}} \Delta P_{TIE12} - \frac{K_{PS1}}{T_{PS}} \Delta P_{DIS1} \quad (4.1)$$

For turbine block in area 1, the equation can be written as

$$\Delta T_{TUR1}^\circ = \frac{1}{\Delta T_{TUR1}} \Delta P_{TUR1} - \frac{1}{\Delta T_{TUR1}} \Delta P_{GEN1} \quad (4.2)$$

For generator side block in area 1, the differential equation is

$$\Delta P_{GEN1}^\circ = -\frac{1}{R_1 T_{GEN1}} \Delta F_1 + \frac{1}{T_{GEN1}} \Delta P_{GEN1} + \frac{1}{T_{GEN1}} \mathbf{u}_1 \quad (4.3)$$

Now, for power system block in area 2

$$\Delta F_2^\circ = -\frac{1}{T_{PS}} \Delta F_2 + \frac{K_{PS2}}{T_{PS}} \Delta P_{TUR2} - \frac{K_{PS2}}{T_{PS}} \Delta P_{TIE12} - \frac{K_{PS2}}{T_{PS}} \Delta P_{DIS2} \quad (4.4)$$

Similarly, for area 2, the equations for turbine block is

$$\Delta T_{TUR2}^\circ = \frac{1}{\Delta T_{TUR2}} \Delta P_{TUR2} - \frac{1}{\Delta T_{TUR2}} \Delta P_{GEN2} \quad (4.5)$$

For generator side block in area 2, the equation becomes

$$\Delta P_{GEN2}^\circ = \frac{1}{R_2 T_{GEN2}} \Delta F_2 - \frac{1}{T_{GEN2}} \Delta P_{GEN2} + \frac{1}{T_{GEN2}} \mathbf{u}_2 \quad (4.6)$$

For tie-line power flow, the equation becomes

$$\Delta P_{TIE12}^\circ = 2\pi t \Delta F_1 - 2\pi t \Delta F_2 \quad (4.7)$$

Now the area control error for area 1 can be written as

$$\mathbf{ACE1} = \mathbf{B}_1 \Delta F_1 (t - t_D) + \Delta P_{TIE12} \quad (4.8)$$

Here t_D is the delay incurred for the loop to the LFC controller part in the form of e^{sT} as shown in the above figures. For the current situation in analysis time delay is taken as zero.

For area 2, the area control can be written as

$$\mathbf{ACE2} = \mathbf{B}_2 \Delta \mathbf{F}_2 (t - t_D) - \Delta \mathbf{P}_{TIE12} \quad (4.9)$$

All the equations from 1- 9 represent the analysis for state variables. Now all the above equations will be arranged in form of matrix represented as state equations.

$$\mathbf{x}^\circ = \mathbf{Ax} + \mathbf{Bu} + \mathbf{Td} \quad (4.10)$$

Where A is state carrying matrix and B is control matrix and d is disturbance matrix considered as negligible.

Now all the above equations are framed in matrix form as shown below.

$$\mathbf{A} = \begin{bmatrix} -\frac{1}{T_{PS}} & \frac{K_{PS1}}{T_{PS}} & 0 & 0 & 0 & 0 & -\frac{K_{PS1}}{T_{PS}} & 0 & 0 \\ 0 & -\frac{1}{\Delta T_{TUR1}} & \frac{1}{\Delta T_{TUR1}} & 0 & 0 & 0 & 0 & 0 & 0 \\ -\frac{1}{R_1 T_{GEN1}} & 0 & \frac{1}{T_{GEN1}} & 0 & 0 & 0 & 0 & 0 & 0 \\ 0 & 0 & 0 & -\frac{1}{T_{PS}} & \frac{K_{PS2}}{T_{PS}} & 0 & -\frac{K_{PS2}}{T_{PS}} & 0 & 0 \\ 0 & 0 & 0 & 0 & -\frac{1}{\Delta T_{TUR2}} & \frac{1}{\Delta T_{TUR2}} & 0 & 0 & 0 \\ 0 & 0 & 0 & \frac{1}{R_2 T_{GEN2}} & 0 & -\frac{1}{T_{GEN2}} & 0 & 0 & 0 \\ 2\pi t & 0 & 0 & -2\pi t & 0 & 0 & 0 & 0 & 0 \\ B_1 & 0 & 0 & 0 & 0 & 0 & 1 & 0 & 0 \\ 0 & 0 & 0 & B_2 & 0 & 0 & -1 & 0 & 0 \end{bmatrix}$$

$$B = \begin{bmatrix} 0 & 0 \\ 0 & 0 \\ \frac{1}{T_{GEN1}} & 0 \\ 0 & 0 \\ 0 & 0 \\ 0 & -\frac{1}{T_{GEN2}} \\ 0 & 0 \\ 0 & 0 \end{bmatrix}$$

Putting the values of each state variables we get to know the stability of developed system. The matrix after putting those values is shown below. These values are further used to find the performance index using Riccati equations. The eigen values calculated from these will let us know how much our developed system is stable, marginally stable or unstable after being applying strategy for developed control system.

$$A = \begin{bmatrix} -.116 & .081 & 0 & 0 & 0 & 0 & -.081 & 0 & 0 \\ 0 & -.111 & .111 & 0 & 0 & 0 & 0 & 0 & 0 \\ -4 & 0 & 4 & 0 & 0 & 0 & 0 & 0 & 0 \\ 0 & 0 & 0 & -.110 & .077 & 0 & -.077 & 0 & 0 \\ 0 & 0 & 0 & 0 & -.111 & .111 & 0 & 0 & 0 \\ 0 & 0 & 0 & 4 & 0 & -4 & 0 & 0 & 0 \\ 1 & 0 & 0 & -1 & 0 & 0 & 0 & 0 & 0 \\ 8 & 0 & 0 & 0 & 0 & 0 & 1 & 0 & 0 \\ 0 & 0 & 0 & 8 & 0 & 0 & -1 & 0 & 0 \end{bmatrix}$$

$$B = \begin{bmatrix} 0 & 0 \\ 0 & 0 \\ 4 & 0 \\ 0 & 0 \\ 0 & 0 \\ 0 & -4 \\ 0 & 0 \\ 0 & 0 \\ 0 & 0 \end{bmatrix}$$

Now we will find state weighting matrix P which is a symmetric, real and positive semi-specific matrix. G is a symmetric, real and positive specific matrix called as control weighting matrix.

The matrices Q and R are resolved on the premise of following system essentials.

1. The perturbations in ACE for steady values have been curtailed. In the above model, these perturbations will be

$$ACE1 = B_1 \Delta F_1 + \Delta P_{TIE12} \quad (4.11)$$

$$ACE2 = B_2 \Delta F_2 - \Delta P_{TIE12} \quad (4.12)$$

2. The perturbations for the control inputs u_1 and u_2 steady values are minimized for all such contemplation, Performance Index will become

$$PI = \frac{1}{2} \int_0^{\infty} [(B_1 x_1 + x_7)^2 + (B_2 - x_7)^2 + (x_8)^2 + (x_9)^2 + (u_1)^2 + (u_2)^2] dt \quad (4.13)$$

This equation will give matrix P and G given below

$$G = \begin{bmatrix} 1 & 0 \\ 0 & 1 \end{bmatrix}$$

$$P = \begin{bmatrix} B_1^2 & 0 & 0 & 0 & 0 & 0 & B_1 & 0 & 0 \\ 0 & 0 & 0 & 0 & 0 & 0 & 0 & 0 & 0 \\ 0 & 0 & 0 & 0 & 0 & 0 & 0 & 0 & 0 \\ 0 & 0 & 0 & B_2^2 & 0 & 0 & -B_2 & 0 & 0 \\ 0 & 0 & 0 & 0 & 0 & 0 & 0 & 0 & 0 \\ 0 & 0 & 0 & 0 & 0 & 0 & 0 & 0 & 0 \\ B_1 & 0 & 0 & -B_2 & 0 & 0 & 2 & 0 & 0 \\ 0 & 0 & 0 & 0 & 0 & 0 & 0 & 1 & 0 \\ 0 & 0 & 0 & 0 & 0 & 0 & 0 & 0 & 1 \end{bmatrix}$$

Where B_1 and $B_2 = 8$ which is symmetric matrix.

Now all the matrices A, B, G, and P are calculated. For optimal control $u = -Kx$ where K is feedback matrix. Using solution for Riccati equations and finding stability of the closed system by calculating eigen values. As per calculated eigen values we are able to conclude about stability. All the calculated matrices are given in appendix section.

Here are few concluding points from state space analysis.

- i. Matrix T is found to be real and symmetric also their eigen values are positive and real.
- ii. The eigen values calculated of matrix A is found that two of its eigen values are zero and the abide have negative real parts presenting that our system is marginally stable.
- iii. The eigen values of N have all negative real parts showing that our system is asymptotically stable.

Programming results and all matrices have been mentioned in the appendix section.

4.3 Conclusion

The main remark for conclusion highlights the developed model with incorporation of communication delay. The delay time included in the system is 0.2 seconds and 0.3 seconds to check frequency impact in both the areas as well as tie line power and results are different than non-incorporation delay. The analysis of communication delay in the system is completed by having zero order of pade approximation. Our system remains at sustained edge till delay of 0.3 seconds. This verifies that propound model can have a stable delay of information signal till 0.3 seconds but with the edge that system takes time to settle down in short some of its oscillations are larger than with non-inclusive nature of delay. The state analysis for propound system has made analysis on the eigen values showing whether the system is marginally stable, asymptotically stable or unstable. For analysis delay is not included as disturbance is also neglected.

CHAPTER 5

SIMULATION RESULTS AND DISCUSSION

5.1 Introduction

Now come to the introduction for the simulation model. The linearized thermal block, linearized LFC block, and linearized vehicle model with the consolidation of wind power in each area. The step load change is 0.01 pu in area 1 and for area 2 is 0.002 pu. The effect of change in load for area 2 is seen in area 1. The propound model shows that reimbursing nature of plugged in vehicles and wind plant had mitigated the power requirement of the system. Results with only PI controller being unstable. Thus, required another control action that mitigates the unstable action. The control system developed to have a gain and integrator block that reduces error till the system becomes stable. The simulation part is incomplete without delay. Also, integral errors have been calculated for each case. The integral error includes errors like integrated absolute error, integrated square error, integrated time absolute error and lastly integrated square time absolute error. These are basically performance indices that give stability nature of any system. The minimum values of these errors indicating stable nature of any system. The penetration effects of vehicle on the system frequency response can be clearly seen in the results section. System frequency analysis also done for 50 % and 70% penetration of plugged vehicles in system. Their responses are different than obtained with 100 % penetration in the system. The control approach applied here is multiple uncertainty control and tuned parameters of PI controller being customized for LFC system. Here Simulink model consist of similar interconnected smart power system with each area consisting of having one thermal power generation, wind power system, vehicle to grid integration and change in load either step or random change in load.

5.3.1 Random Change of Wind Speed for Step Change in load

With conventional controller, propound system results are shown in this section. This figure has wind speed given to the wind power plant.

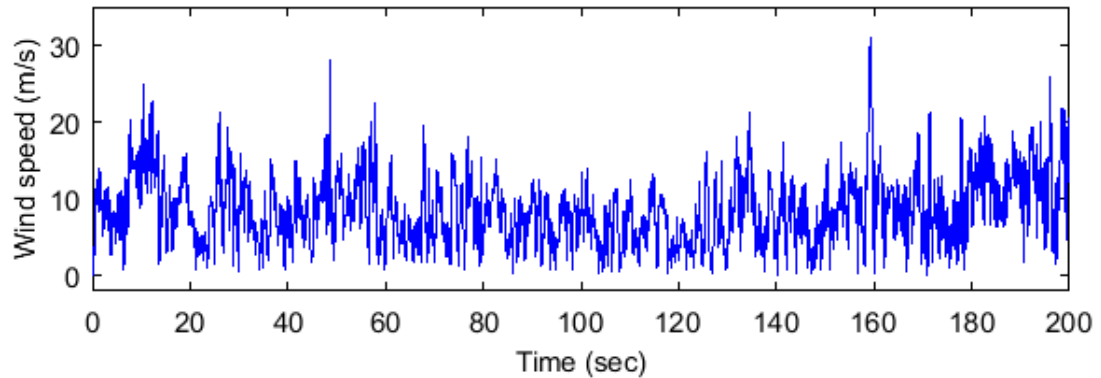


Figure 5.2: Wind speed given to wind plant

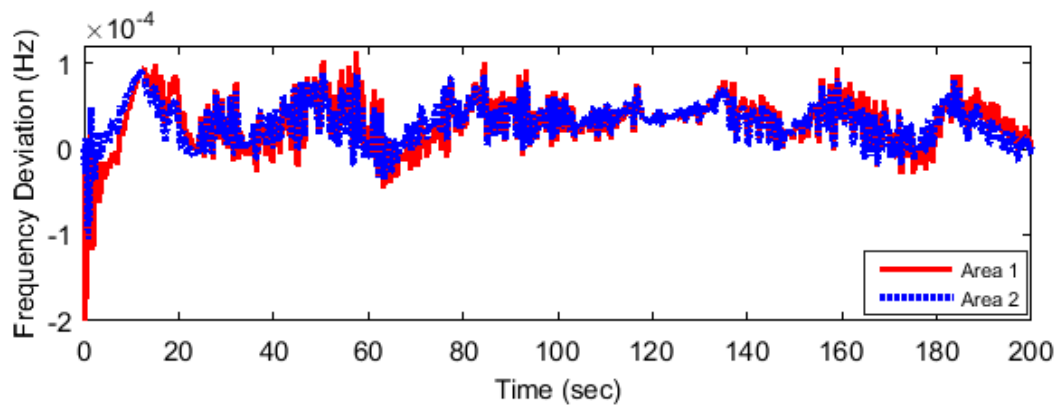


Figure 5.3: System frequency response with PI controller with random wind speed

The above label showing us response about frequency aberration with PI controller in action for the two-area system. As we can see that system has not being settled resulting in large settling time and maximum shoot out in results.

5.3.2 Step Change of Wind Speed for Step Change in Load

The second case with PI controller show results with step load in change for step change for wind speed given to propound system. For area 1 step load in change is 0.01 per unit and in area 2 step load in change is 0.002 per unit.

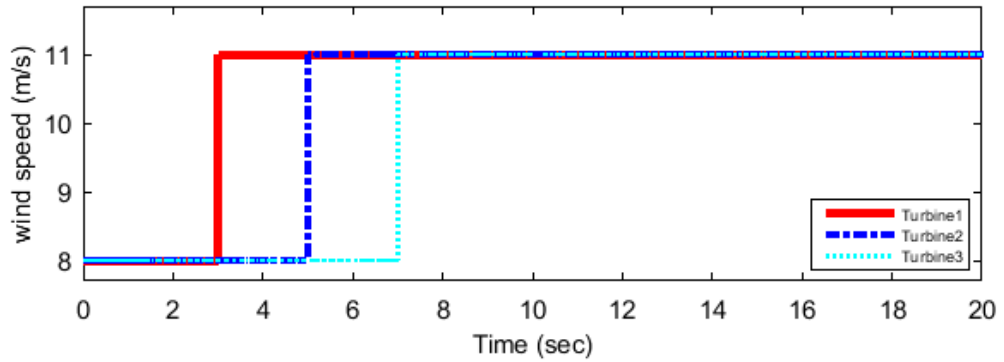


Figure 5.4: Step change in wind speed given to system

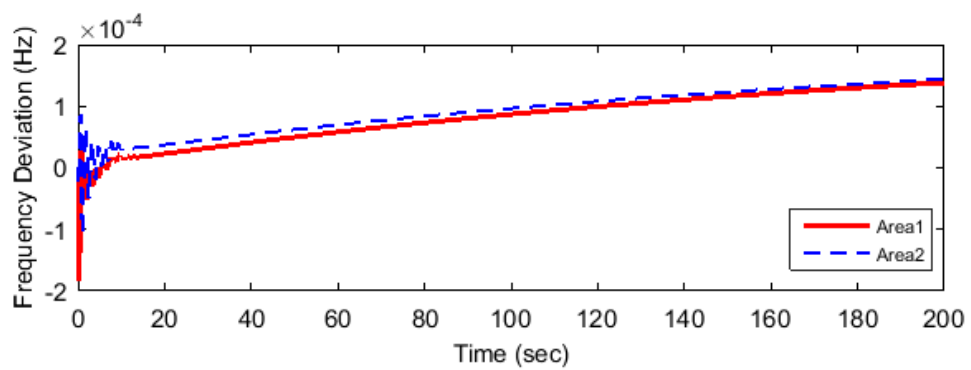


Figure 5.5: System frequency response with PI controller with step wind speed

Above label showing the response with PI controller with step change in wind speed. Clearly PI controller is not sufficient to make better system response. As figure showing results with increasing deviation of frequency with gradual simulation time. It shows system never settle down till the simulation time and clearly the result being unstable for the incorporated PI controller.

5.3.3 Step Change in Wind Speed with Random Change in Load

The third case is for the same step wind speed but with random change in load. The random signal for both the signal is given below.

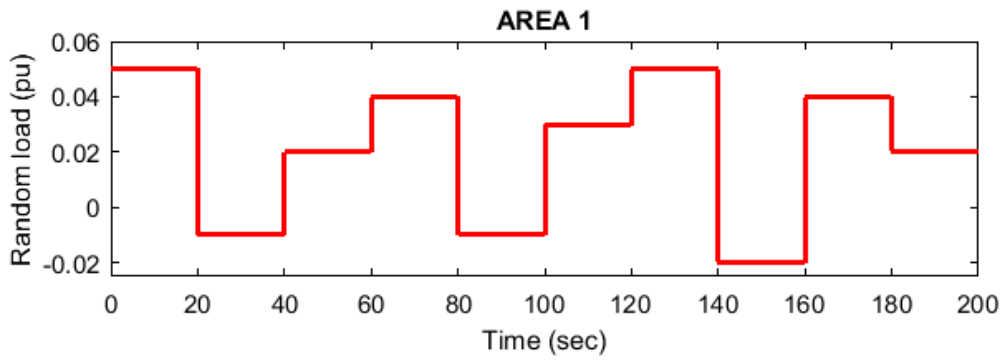


Figure 5.6: System response with random change in load in area 1

This label showing random change in load that has been applied to area 1. A kind of random change in load was applied with the step change in wind speed.

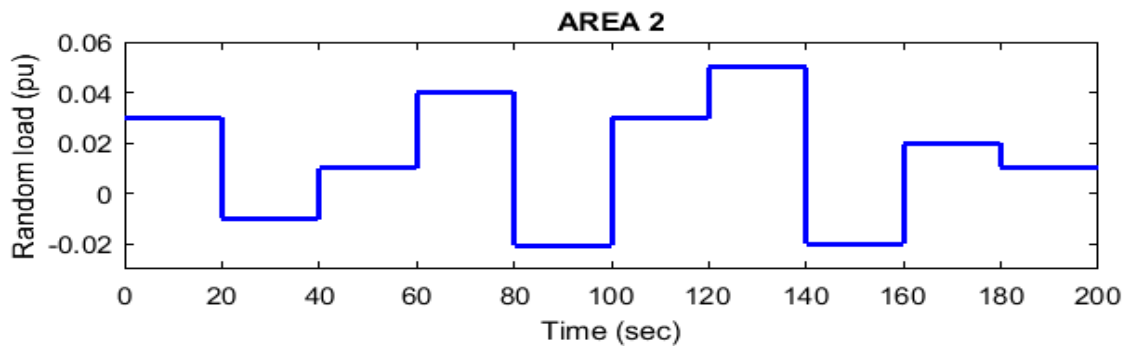


Figure 5.7: System response with random change in load in area 2

This label has given us idea about random load given in area 2 for the propound system.

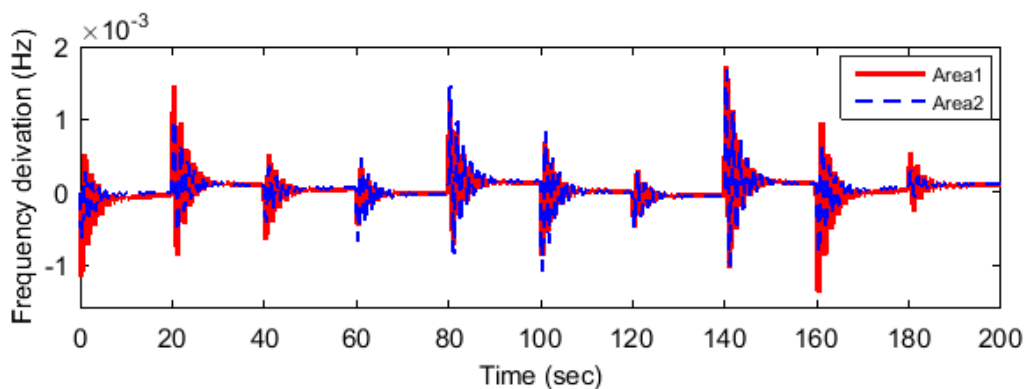


Figure 5.8: System response with PI controller with random change in load

The label shows unstable nature of two area system, as system is not stable with using PI controller. Thus, required another control action.

5.4 Performance of the System with H_∞ controller

The results obtained by the conventional controller are not stable. Thus, another control action is required. This control implemented is control of system with multiple uncertainty. For this same three cases have been adopted to check system response.

5.4.1 Random Change of Wind Speed for Step Change in load

The wind signal given for this case is same given in first case of PI controller. But in this case the controller used is multiple uncertainty control.

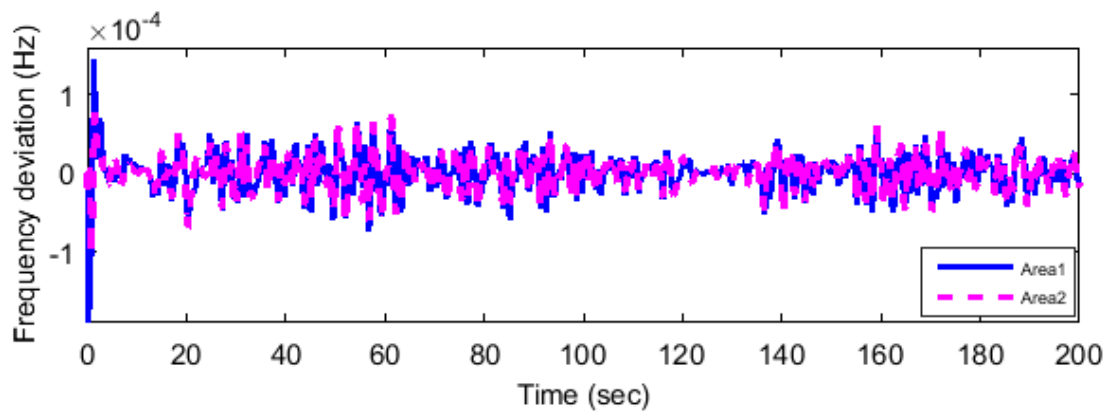


Figure 5.9: System frequency response with H_∞ controller with random change in wind speed

Above labels showing deviations in frequency of both areas connected to each other. The frequency perturbations are as minimum as shown in figure. As our wind signal is changeable at every second, thus resulting in changeable frequency signal.

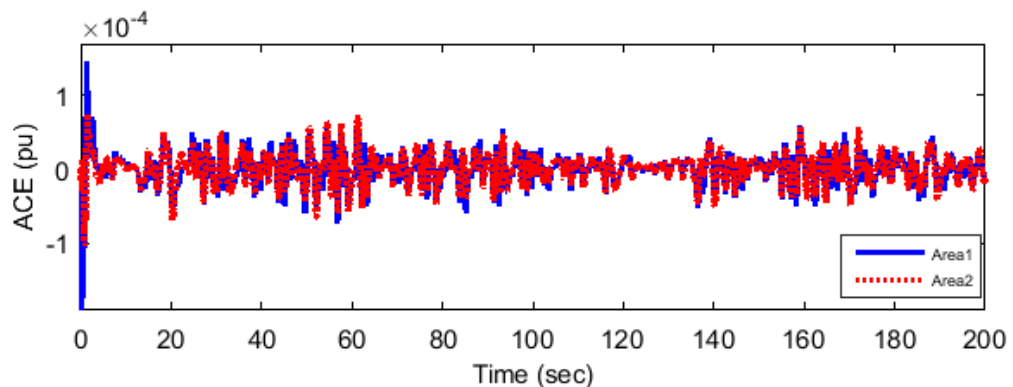


Figure 5.10: System area control error response with H_∞ controller with random change in wind speed

This label is giving us idea about area control error in both the areas with minimum perturbations as PI controller is in use. As frequency of both areas are varying continuously because wind speed is varying continuous in nature.

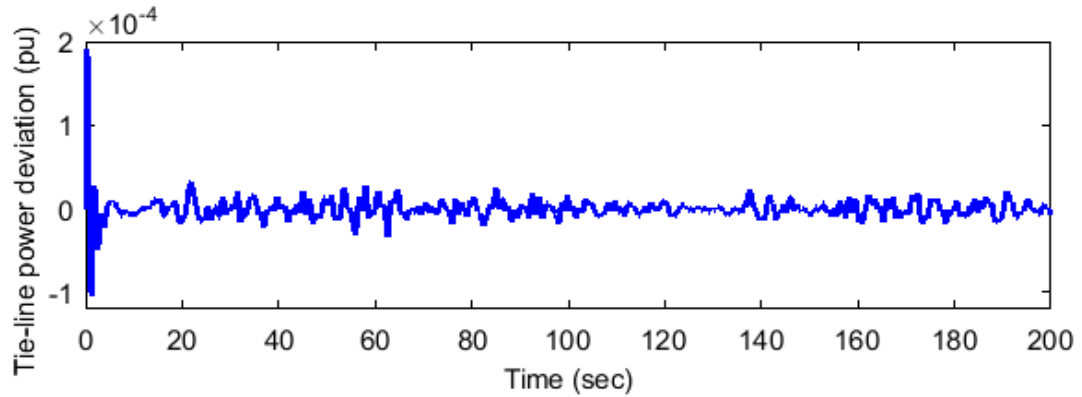


Figure 5.11: System tie-line power response with H_∞ controller with random change in wind speed

Tie-line power also seems to be of varying nature because of continuous changing wind speed for the particular simulation time. As controller action takes place the power in tie line has deviations within bound.

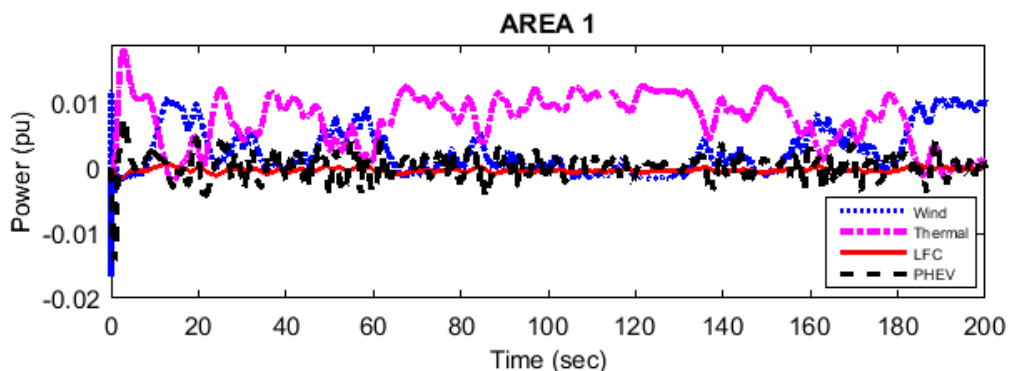


Figure 5.12: Power capacity in area 1 with H_∞ controller with random change in wind speed

The per unit power of each unit is being present in above figure. As we can see that thermal plant has been dominating over other units providing power for compensation of load demand in the area 1. The labels of power capacity of area 1 and area 2 showing dominating nature of thermal power with the contribution of wind power.

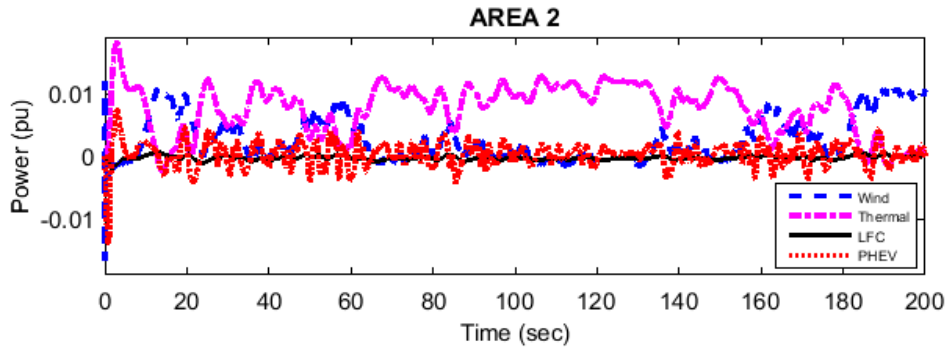


Figure 5.13: Power capacity in area 2 with H_∞ controller with random change in wind speed

This label showing per unit power of each unit. As we can see that thermal plant has been dominating over other units providing power for compensation of load demand in the area 2. All the results obtained with this case are stable in proved better than results obtained from PI controller. Thus, our developed control scheme is best to mitigate the unstable nature of system than using the PI controller only.

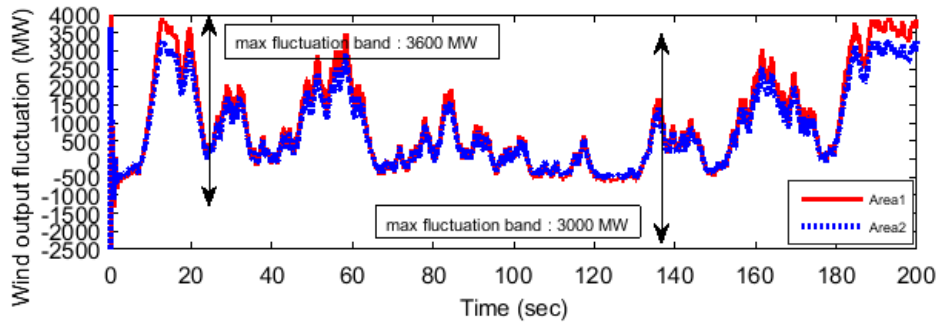


Figure 5.14: Wind power output (MW) with H_∞ controller with random change in wind speed

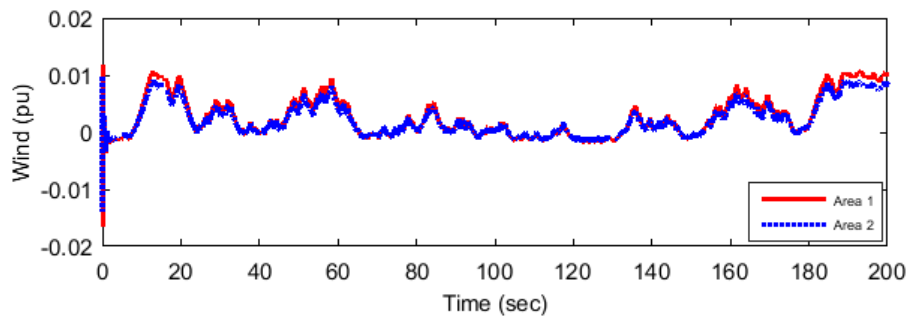


Figure 5.15: Wind power output (pu) with H_∞ controller with random change in wind speed

The above presented labels give idea of generated power capacity (MW) of wind power plant which is incorporated the propound system. For the developed system, this megawatt power is converted into per unit power. Thus, working of propound

system is in per unit system. In label 5.14 maximum and minimum fluctuations of megawatt power is shown.

5.4.2 Step Change of Wind Speed for Step Change in Load

Label below showing response of frequency of both the areas. As the simulation time is 200 seconds, but the figure is showing results with 20 seconds. Clearly the system is settled within 20 seconds showing accurate working of PI controller. The control scheme applied is proved best for system.

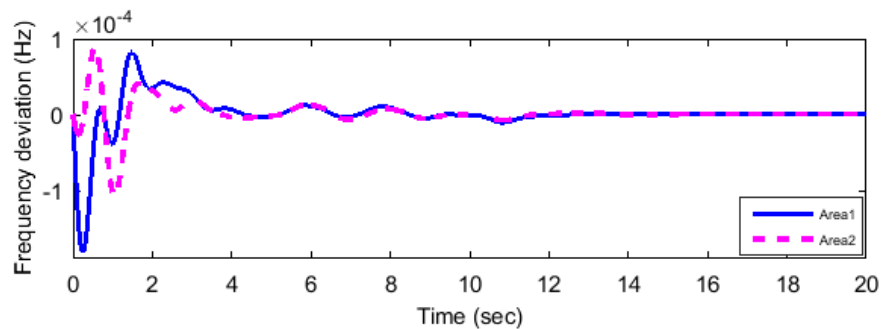


Figure 5.16: System frequency response with H_{∞} controller with step wind speed

The above label is showing response of frequency perturbations for the step change in wind speed with the step change in load. The simulation time for the response is 200 seconds but for clear visible response the label showing response for 20s. As we can see that system is settled within time frame of 20s, thus proposed system is stable.

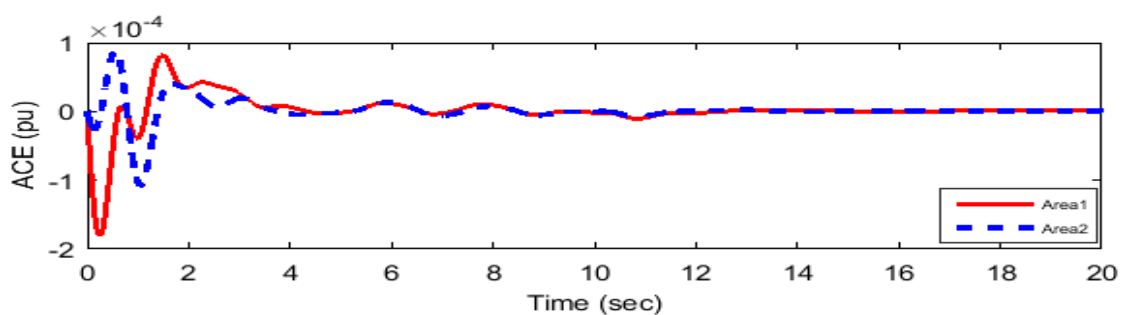


Figure 5.17: System area control response with H_{∞} controller with step wind speed

System response showing results for area control error showing stability of system within less time of operation of composite power system. As the simulation time for the system is 200 seconds, but the figure is showing results with 20 seconds. Thus, our proposed system is working for accuracy in results.

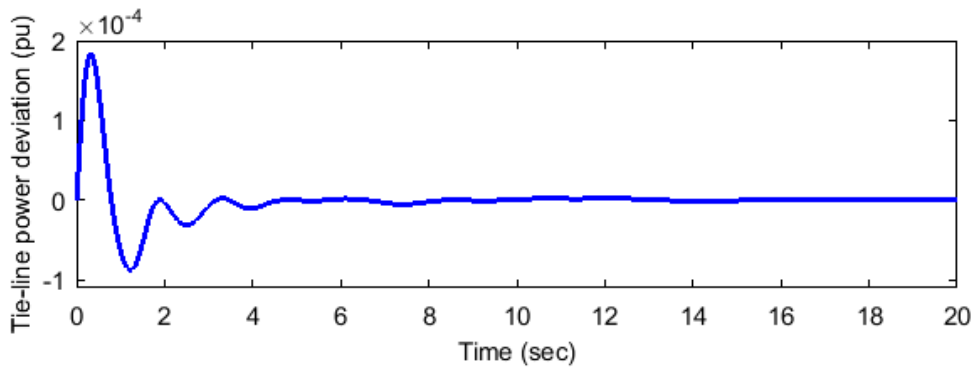


Figure 5.18: System tie-line power response with H_∞ controller with step wind speed

This label is presenting deviations in tie line power for step load in change. As perturbations are settled within few seconds of time. The whole simulation time is 200 seconds for every label included over here. For perfection in labels, some are shown only with 20 seconds of time.

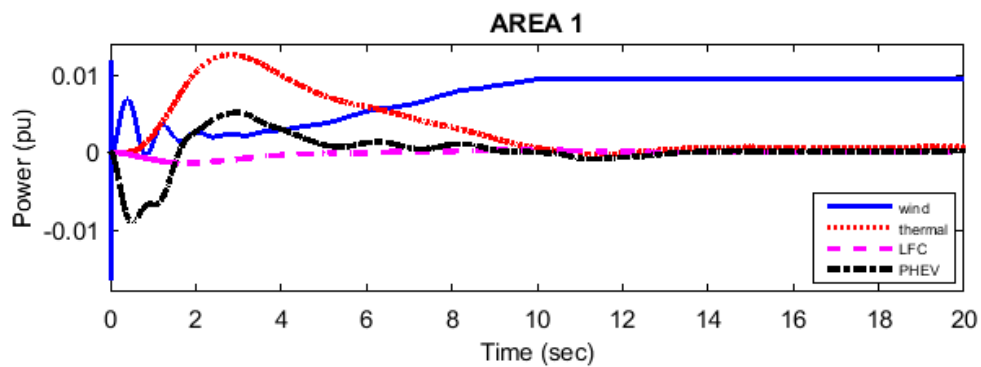


Figure 5.19: Power capacity in area 1 with H_∞ controller with step wind speed

Above labels are presenting the per unit power capacity in area 2 for the propound system. As we can see that for step load in change, power of thermal plant is dominating the other power contributors. This presented label is showing per unit power capacities for all the integrated structures showing that wind power is being dominating over other incorporated systems. Thus, concluded for a step change in wind speed, with the step load only power from wind can reimburse the connected system.

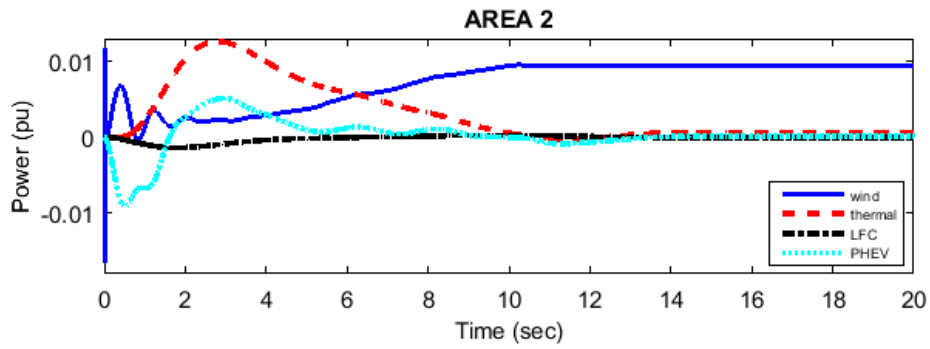


Figure 5.20: Power capacity in area 2 with H_{∞} controller with step wind speed

Above labels are presenting the per unit power capacity in area 2 for the propound system. As we can see that for step load in change, power of thermal plant is dominating the other power contributors. Similarly, for the area 2, power from wind is dominating the other interlinked sources. For the step load wind power has reimburse the required power in the propound system.

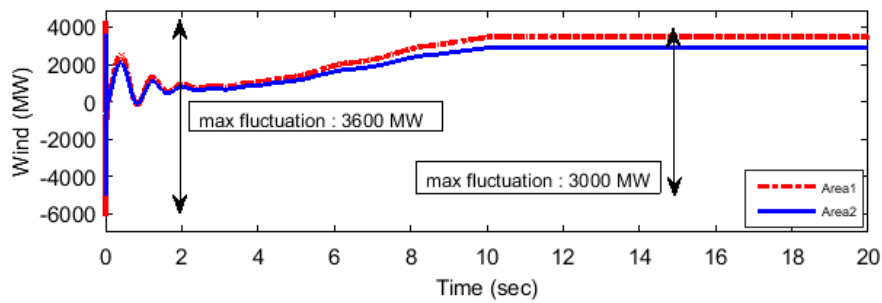


Figure 5.21: Wind power capacity (MW) with H_{∞} controller with step wind speed

Here is the label for wind power capacity in MW. Figure showing maximum fluctuations for both the studied system areas. Area 1 is giving power capacity about 3600 MW while area 2 is giving 3000 MW power to the system.

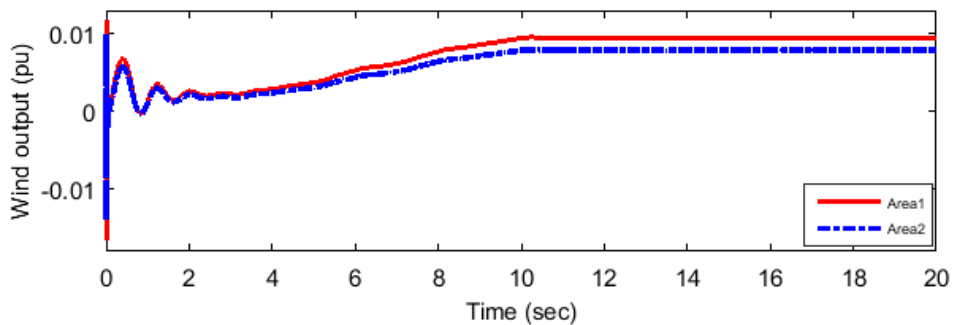


Figure 5.22: Wind power capacity (pu) with H_{∞} controller with step wind speed

My proposed system is per unit system so megawatt power from wind plant is converted into pu power to make system to work in per unit system.

5.4.3 Step Change of Wind Speed for Random Change in Load

The random load is given for both the areas. Now have results with random change in load with the same step wind speed.

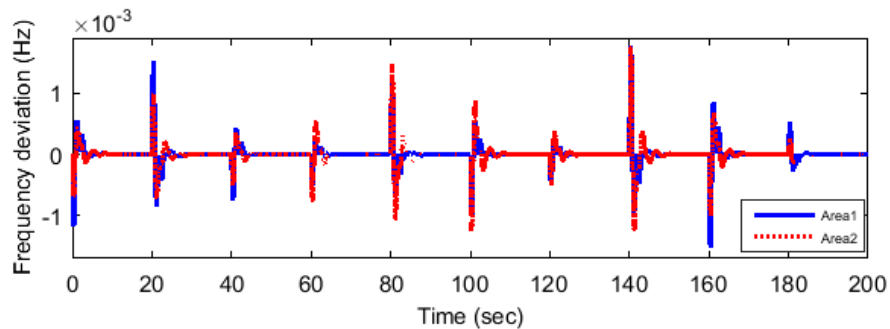


Figure 5.23: System frequency response with H_{∞} controller with random change in load

This label showing response with deviations in frequency for both the studied areas of the interconnected system. This is indeed due to the random change in load which affects the frequency of the system for a particular change in the signal.

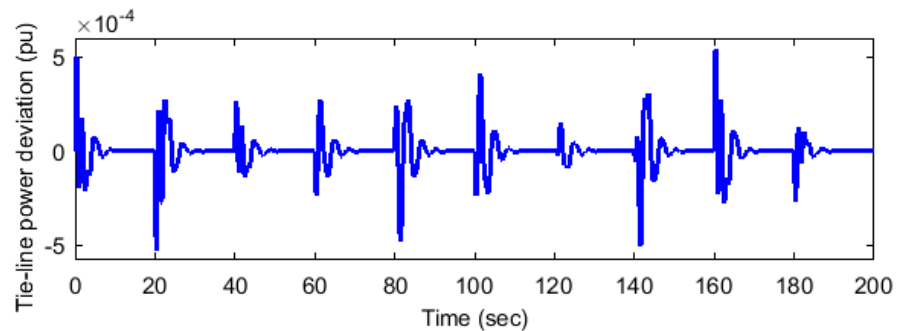


Figure 5.24: System tie-line power response with H_{∞} controller with random change in load

Both the above label has the frequency extrusions response and the tie-line power response. As we can see from the area 1 and area 2 load figure, it is visible that the where the signal is changing there is deviations in the frequency of both the studied areas as well as the tie line power flow deviations. Other than step change in load and random change in wind speed cases for this case the tie line power deviation is more than other two.

5.5 Comparison Based on Performance of PI and H_∞ Controller

The comparison of both of the controllers are shown below. The results produced with H_∞ Controller are better than conventional controller.

5.5.1 Random Change of Wind Speed for Step Change in load

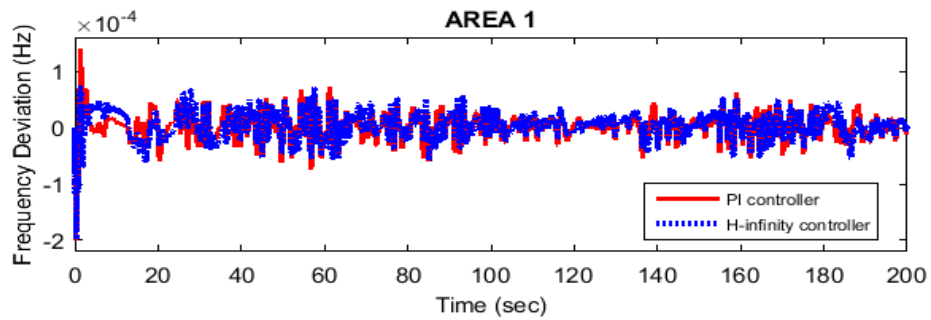


Figure 5.25: System frequency response with comparison of controllers for area 1

System frequency response comparing performance for both the controllers. With PI controller oscillations are more.

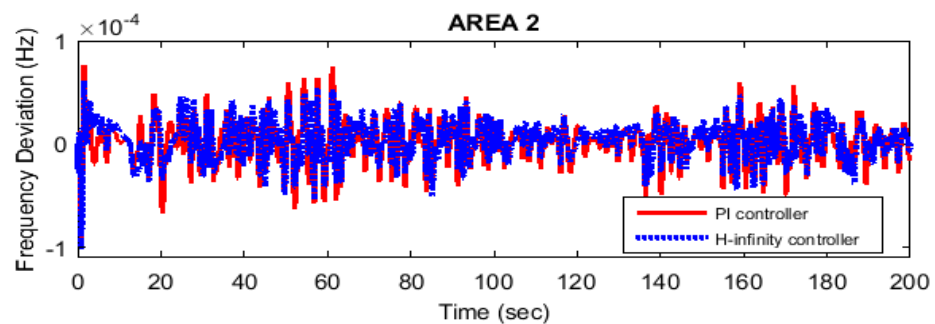


Figure 5.26: System frequency response with comparison of controllers for area 2

5.5.2 Step Change of Wind Speed for Step Change in load

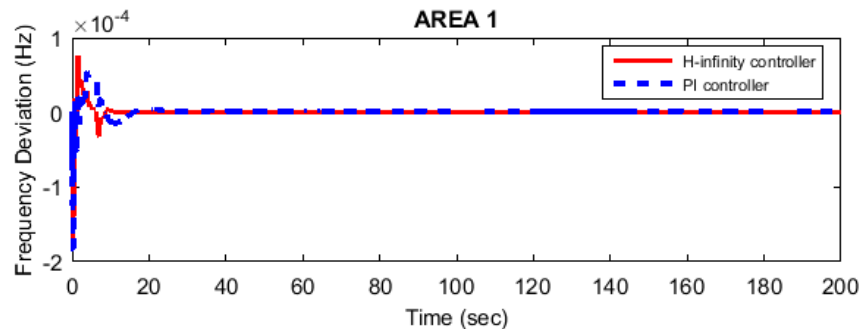


Figure 5.27: System frequency response for area 1 with step change in wind speed

The response of area 1 with both the controllers for step change in load with step change in wind speed had shown in above label.

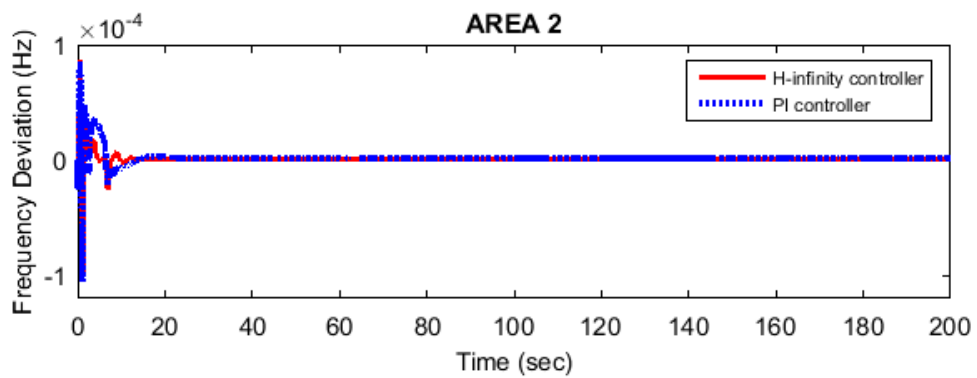


Figure 5.28: System frequency response for area 2 with step change in wind speed

5.5.3 Step Change of Wind Speed for Random Change in load

The response for random change in load with step change in wind speed have been shown in the next figure.

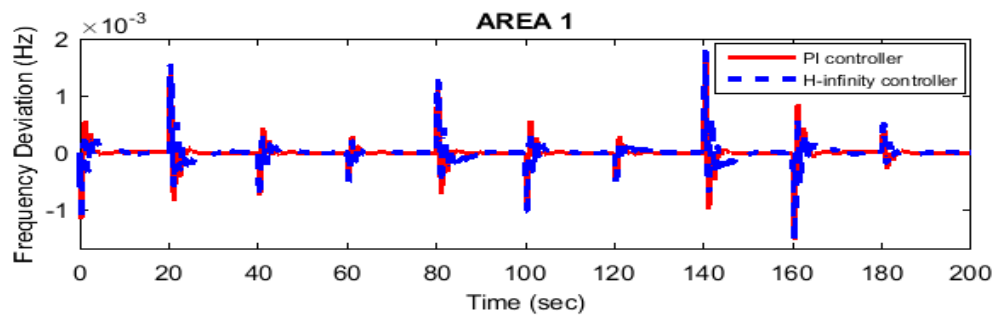


Figure 5.29: System frequency response for area 1 with random change in load

The response of both the controllers have been shown here.

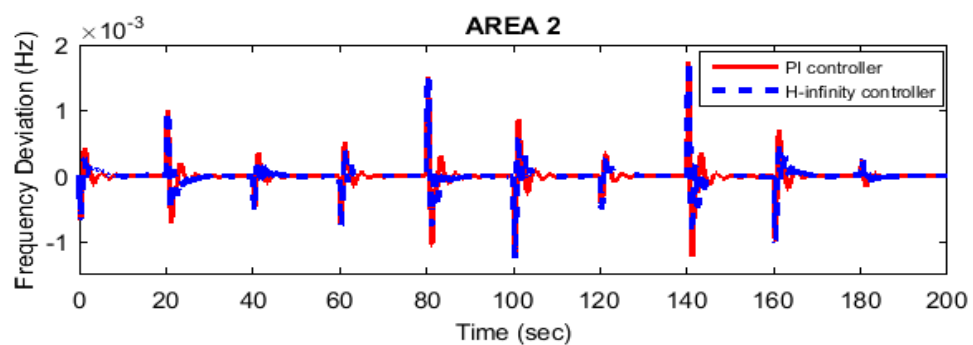


Figure 5.30: System frequency response for area 2 with random change in load

The above label is showing system frequency response in area 2 with minimum deviations for H_∞ controller. The oscillations with PI controller are more than with H_∞ controller. The rise time and settling time with H_∞ controller is smaller than PI controller. The proposed system settles down early with H_∞ controller but with PI controller takes time to settle for the proposed system. This shows robustness of the proposed H_∞ controller.

5.6 Performance of the System with Communication Delay

This section includes the results with delay incorporation. Starting with the first case given below. This result obtained with delay are different from non-incorporation of delay.

5.6.1 Random Change of Wind Speed for Step Change in load

Now coming to the introduction of delay in our system. After the introduction of delay, we are able to make some points about fact that delay does affect stability of our system. The figure on the next page showing the effects of delay in our system and are compared for analyzing results obtained without controller. Results with communication delay have large oscillations in the proposed system

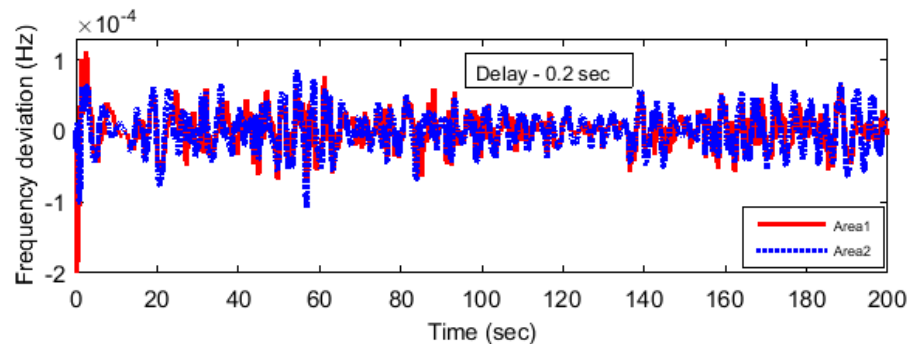


Figure 5.31: System frequency response after delay of 0.2 seconds with random change in wind speed

It is clearly visible that system settling time has been risen up and as well as maximum shoot up of system. Even delay of 0.2 seconds can make such a difference for stable system. Thus, our controller part here needs to be robust for such extreme deviations in developed system.

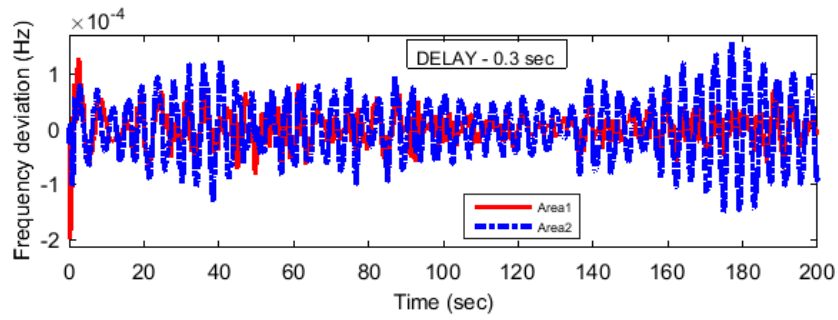


Figure 5.32: System frequency response after delay of 0.3 seconds with random change in wind speed

As the delay time increases directly affecting system firmness. On comparing both the above figures we can conclude that as the delay time is increased it hampers the stable system. For this most important part is of controller to make our system leads to being collapsed.

5.6.2 Step Change of Wind Speed for Step Change in Load

The results shown on the next page have step wind speed but with step load in change and are different. The next 2 figures will be showing results with incorporating delay in the proposed and studied system. Delay of few seconds will be to check frequency responses for both the connected areas of the studied system.

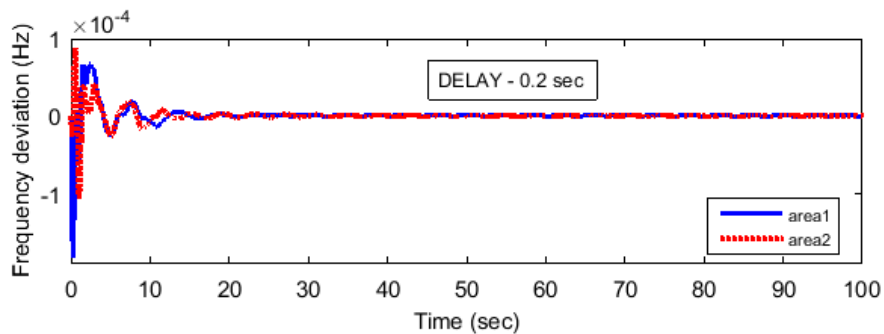


Figure 5.33: System frequency response incorporating delay of 0.2 seconds with step wind speed

The label above is showing results against delay of few seconds. As system is not being settled for the simulation time of 200 seconds, but display figure is showing up to 100 seconds result. It shows that delay has impact on stability of developed system and frequency fluctuations are there in the system. it shows that system is not stable.

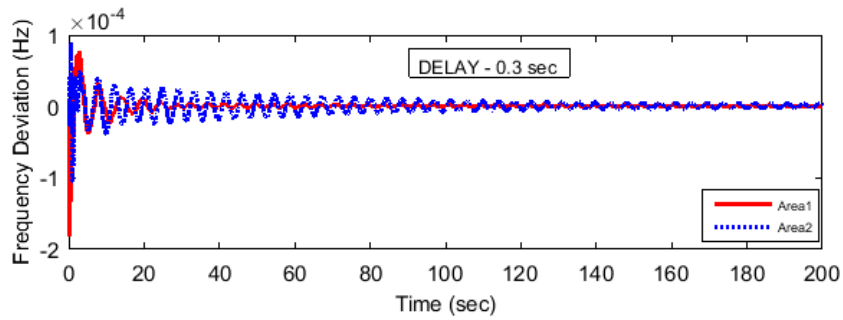


Figure 5.34: System frequency response incorporating delay of .3 seconds with step wind speed

Above label have the inclusion of delay. For change in step load with the step change in wind speed, the system becomes completely unstable and fluctuations are there in simulation time for system. We can conclude from this figure that after the delay of 0.35 seconds the can become completely unstable. Thus, it needs to be ensure that for step load not more than .3 seconds can be encouraged in the system otherwise leads to completely shut down of system due to delay of exchanged information.

5.6.3 Step Change of Wind Speed for Random Change in Load

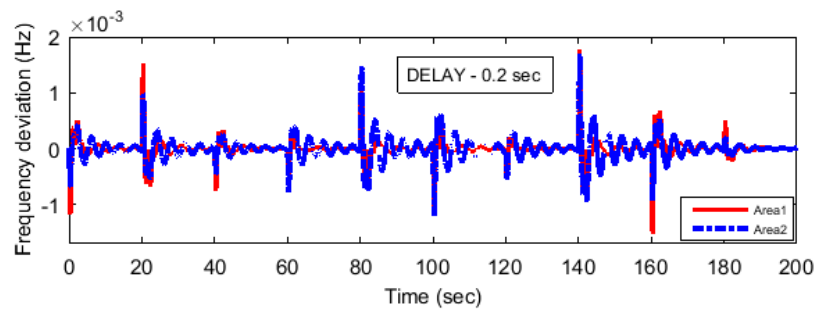


Figure 5.35: Frequency response with delay of 0.2 seconds with random change in load

This label showing results obtained from random change in load with the incorporation of communication delay of 0.2 seconds in the studied system. As we can see that due to delay inclusion the frequency response has been different has system is taking more time to settle down as well system shoot up is more than without delay figures.

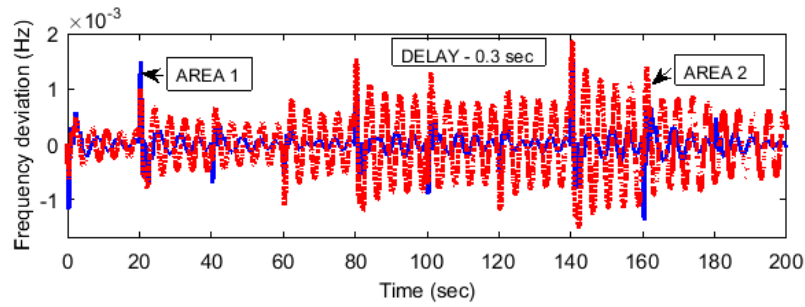


Figure 5.36: Frequency response with delay of 0.3 seconds with random change in load

The label including delay has large frequency deviations in the system as well as the system has not been settled and deviations are not being settled this shows the damping effect of delay. It can be concluded that for random case if delay time is increased to another second then system might become completely unstable if further delay is present in the system.

5.7 Performance of System with Different Penetration of Electric Vehicle

5.7.1 Random Change of Wind Speed for Step Change in load

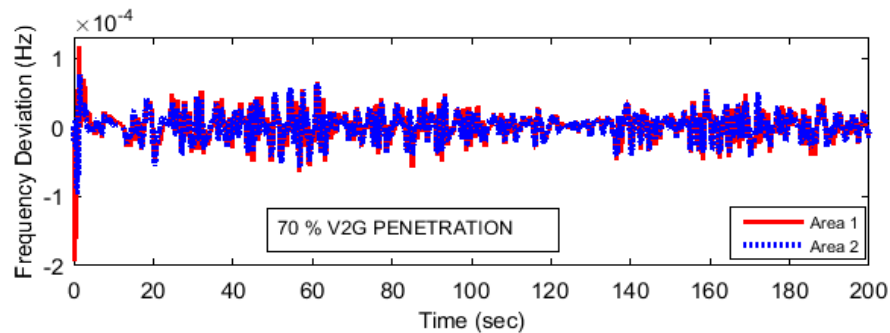


Figure 5.37: System frequency response at 70 % V2G penetration with random change in wind speed

Here is the label showing V2G penetration in the system connected with wind plant, thermal plant. At 70 % penetration of vehicle stored power is being utilized here in system. it is different from 100 % penetration of all other figures above this figure.

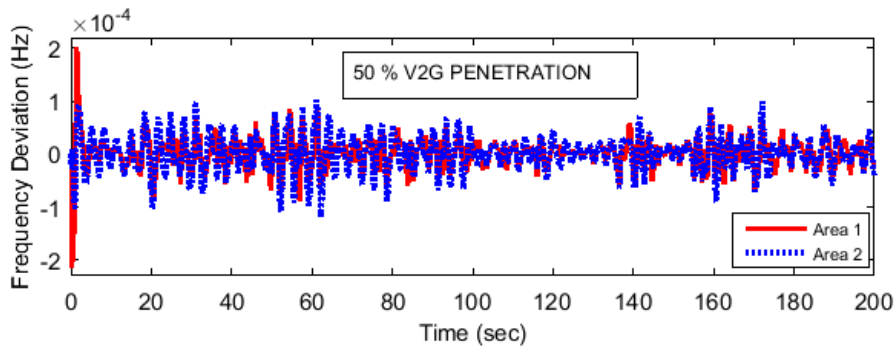


Figure 5.38: System frequency response at 50 % V2G penetration with random change in wind speed

This label is showing only 50 % of its utilization in the system. Clearly showing the effects on frequency of the both areas. Thus, results with 50 %, 70% and 100% are different showing response in different cases of the smart grid. This kind of research has made us to conclude that V2G power penetration do affect our system presentation whenever non-exhaustible energy resources are unsegregated to traditional systems of thermal, hydro etc.

5.7.2 Step Change of Wind Speed for Step Change in Load

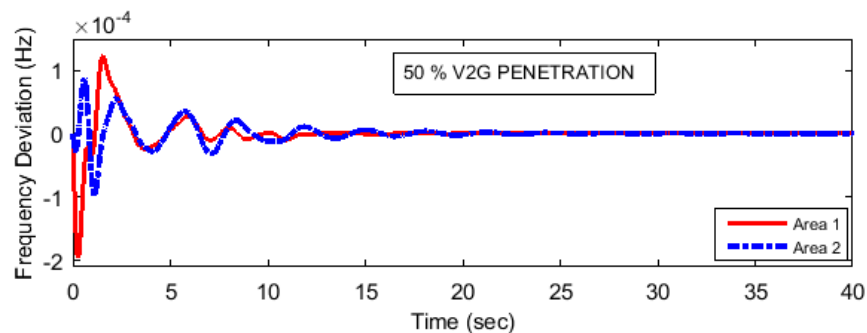


Figure 5.39: System frequency response at 50 % V2G penetration with step wind speed

This label showing response with only 50 % V2G penetration in the proposed system. The system is taking time to settle down but the simulation time for the system is 200 seconds. For the figure purpose the time is eventually taken as 40 seconds for clear vision of the response taken.

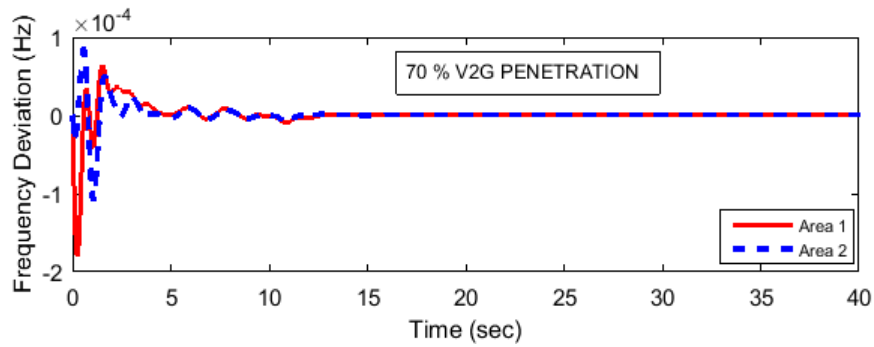


Figure 5.40: System frequency response at 70 % V2G penetration with step wind speed

The above label has response for 70 % V2G penetration in the system. As we can see that this result is entirely different from 50 % V2G penetration and 100 % V2G penetration. At 70 % V2G power penetration is settled near about 13 seconds of simulation time. The result is taken for 40 seconds for showing difference between 50% and 70 % V2G power penetration. The whole system has made to run over 200 seconds of time but for result purpose it has reduced time scale to 40 seconds.

5.7.3 Step Change of Wind Speed for Random Change in Load

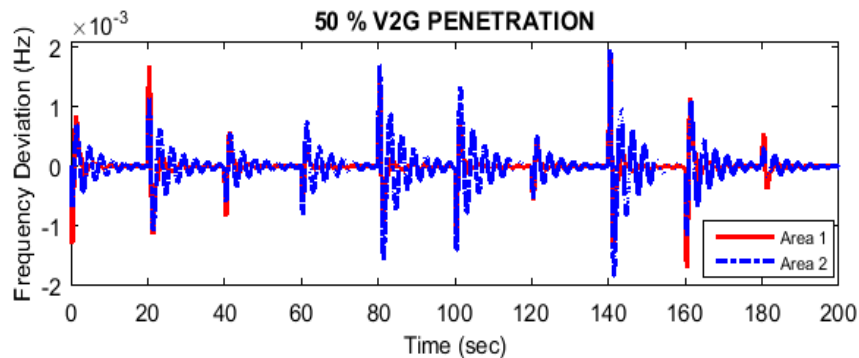


Figure 5.41: System frequency response at 50 % V2G penetration with random change in load

The label results have V2G penetration of about 50 % in the system. This response has been different from the 100 % penetration of V2G taken for all the 3 cases.

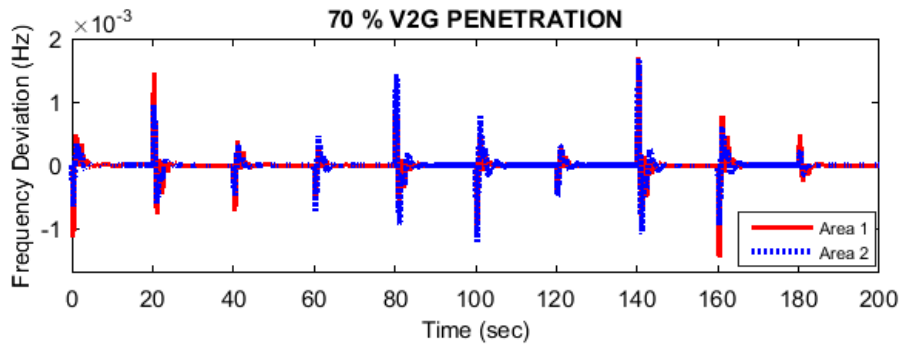


Figure 5.42: System frequency response at 70 % V2G penetration with random change in load

The label showing 70 % V2G penetration in the studied system. The figure giving responses for different stages of V2G penetration and for all the three cases are proved to be different in all aspects.

5.8 Performance Indices

Table 5.1: Random Wind Speed for Step Change in Load

PERFORMANCE INDICES	AREA 1	AREA 2
Integrated Square Error (ISE)	1.179×10^7	8.432×10^{-8}
Integrated Absolute Error (IAE)	.003559	.003125
Integrated Time Absolute Error (ITAE)	0.3223	0.2932
Integrated Square Time Absolute Error (ISTAE)	.00103	.008914

Table 5.2: Step Wind Speed for Step Change in Load

PERFORMANCE INDICES	AREA 1	AREA 2
Integrated Square Error (ISE)	1.405×10^{-8}	6.835×10^{-9}
Integrated Absolute Error (IAE)	.0003755	.0003205
Integrated Time Absolute Error (ITAE)	0.01878	0.01867
Integrated Square Time Absolute Error (ISTAE)	2.275×10^{-6}	2.262×10^{-6}

Table 5.3: Step Wind Speed for Random Change in Load

PERFORMANCE INDICES	AREA 1	AREA 2
Integrated Square Error (ISE)	7.22×10^{-3}	7.231×10^{-6}
Integrated Absolute Error (IAE)	.01142	.01316
Integrated Time Absolute Error (ITAE)	1.036	1.226
Integrated Square Time Absolute Error (ISTAE)	.08744	.08691

5.9 Conclusion

At the end of the results chapter, conclusions recognized proved the system behavior with all the cases obliged in the system. The results produced using PI controller lack of mitigating nature, while the proposed controller of multiple uncertainty have better response of frequency, tie line power and area control error of identical system. the proposed H_{∞} Controller has an edge over PI controller in the form of results obtained. Thus, response from H_{∞} Controller is better than conventional controller. Incorporating delay have made some changes in the response than obtained earlier. After delay, system comes across large frequency oscillations. Propound system has sustained minimum frequency deviations for the simulation time up to 0.3 seconds. Similarly, in the case of showing different penetration effects of vehicle has analyzed with the frequency response only for the case when there is only 50 % penetration of vehicle power and other is when there is 70 % perforation of vehicle power in the identical system. All the cases presented here like random wind speed with step in load, step wind speed with step change in load and lastly step wind speed with random change in load have different aspects of their results and completely justify the proposed controller work for identical power system.

CHAPTER 6

CONCLUSION AND FUTURE SCOPE

6.1 Conclusion

Two area hybrid power system is proposed for thesis. The non-exhaustible energy resources have been incorporated in the system because of the non-reimbursement of the power in the conventional power system. the vehicle to grid model has fast damping result than the thermal plant that is why vehicle model is used to recompense the adequate amount of power requirement in the proposed system. The controller proposed for the system has got much better response than the conventional (PI) controller. The communication delay has been incorporated in the system to have pronounced effect on frequency, tie line power and area control error. The loss of information in the propound system is the delay of signals carrying information in the system. This affects frequency breach of the system. The per unit system has got results within minimal perturbation of frequency, area control error and tie line frequency deviations. The results shown in previous chapter has clearly made some conclusions that effect of wind and PHEV can be clearly seen. Different loads have been applied to system and different wind signals were used to check the frequency response, area control error, tie-line power, and power capacity in both areas. When real wind signal was applied the thermal power, plant was more dominating than wind, PHEV and LFC. When random load was given to both areas with base wind speed of 11 m/s then PHEV was dominating the system and similarly when the step load was applied clearly wind plant was dominating in the system. The step perturbation of load in area 1 was 0.01 pu and in area 2 it was 0.002 pu. Different perspectives made by applying all of them. During step change in load the system settled within 20s designating that the system is stable.

Clearly the capacity of LFC is reimbursed by applying the wind power plant and the PHEV power. This has made me clear that the smart grid is really a need for future power system. The perspective of smarter grid has been clearly visible in the results produced from my work. The scenario presented in my report is completely justifying by results which has been presented in previous chapters.

Some results with focus on the effects of communication delay which has been implemented with system. This has made us clear that communication information delay can hamper system stability to a greater extent if not detected earlier.

6.2 Future Scope

1. Rate of revise of frequency can also be estimated with false data can be boosted within system model to work for cyber security of developed system.
2. Multi area power system for future works can be incorporated with the integration of other than wind and hybrid vehicles. This model can be elongated to multi area power system with the latest optimization execution.
3. There is requirement of robust frequency controller for large communication delay in system. Better control proficiency can be developed incorporating latest sliding controllers.

PUBLICATIONS

- [1] Rushil Sagotra, Manoj Badoni, Vijay P. Singh, and Navdeep Singh, “Frequency regulation of interconnected power system in perspective of smart grid environment,” *International Journal of Electronics, Electrical and Computational System (IIEECS), Academic Science*, vol.7, Issue 5, pp.109–117, May 2018.

REFERENCES

- [1] S. A. Pourmousavi, M. H. Nehrir, “Introducing dynamic demand response in the LFC Model,” *IEEE Trans. Power Syst.*, vol.29, no.4, pp. 1562–1572, Jul. 2014.
- [2] K. Moslehi, R. Kumar, “A reliability perspective of the smart grid,” *IEEE Trans. Smart Grid*, vol.1 no.1, pp. 57–64, Jun.2010.
- [3] A. Y. Saber, G. K. Vengayamoothy, “Plug-in vehicles and renewable energy sources for cost and emission reductions,” *IEEE Trans. on Industrial Elect.*, vol. 58, no.4, pp. 1229–1238, Apr. 2011.
- [4] E. Sortomme, M. M. Hindi, S. D. James MacPherson, and S.S. Venkata, “Coordinating vehicle-to-grid service with energy trading,” *IEEE Trans. Smart Grid*, vol. 3, no. 1, pp. 453–462, Mar. 2012.
- [5] Y. Huang, S. Werner, J. Huang, N. Kashyap, and V. Gupta, “State estimation in electric power grids: Meeting new challenges presented by the requirements of the future grid,” *IEEE Signal Processing Magazine*, vol. 29, no. 5, pp. 33–43, Sep. 2012.
- [6] Y. Ota, H. Taniguchi, T. Nakajima, K. M. Liyanage, J. Baba, and A. Yokoyama, “Autonomous distributed V2G (vehicle-to-grid) satisfying scheduled charging,” *IEEE Trans. Smart Grid*, vol. 3, no. 1, pp. 559–564, Mar. 2012.
- [7] M. Aunedi, P. A. Kountouriotis, J. E. Ortega Calderon, D. Angeli, and G. Strbac, “Economic and environmental benefits of dynamic demand in providing frequency regulation,” *IEEE Trans. Smart Grid*, vol. 4, no. 4, pp. 2036–2048, Dec. 2013.
- [8] S. Weckx, R. D'Hulst, and J. Driesen, “Primary and secondary frequency support by a multi-agent demand control system,” *IEEE Trans. Power Syst.*, vol.30, no.3, pp. 1394–1404, May. 2015.
- [9] Z. Akhtar, B. Chaudhuri, and S. Y. R. Hui, “Primary frequency control contribution from smart loads using reactive compensation,” *IEEE Trans. Smart Grid*, vol. 6, no. 5, pp. 2356–2365, Sep. 2015.

- [10] H. Bevrani, A. Ghosh, G. Ledwich, “Renewable energy sources and frequency regulation: survey and new perspectives,” *IET Renew. Power Gener.*, vol.4, no.5, pp. 438–457, May. 2016.
- [11] A. Z. Alireza, T. Mohammadreza, R. A. Mohammad, “Coordinated design of fuzzy-based speed controller and auxiliary controllers in available speed wind turbine to enhance frequency control,” *IET Renew. Power Gener.*, vol.10, no.9, pp. 1298–1308, May. 2016.
- [12] E. Y. K. Nour, M. Mohamed, H. Mourad, B. Mohamed, “LFC enhancement concerning large wind power integration using new optimised PID controller and RFBs,” *IET Gener. Trans. Distrib.*, vol. 6, no.4, pp. 4065–4077, Jul. 2016.
- [13] X. Liu, Y. Zhang, and K. Lee, “Coordinated distributed MPC for load frequency control of power system with wind farms,” *IEEE Trans. Ind. Elect.*, vol. 54, no.6, pp. 5140–5150, Jun. 2017.
- [14] K. Liao, and Y. Xu, “A robust load frequency control scheme for power systems Based on second-order sliding mode and extended disturbance observer,” *IEEE Trans. Ind. Informat.*, Nov. 2017.
- [15] Z. X. Zou, G. D. Carne, G. Buticchi, and M. Liserre, “Frequency-adaptive control of smart transformer-fed distribution grid,” *IEEE Trans. Ind. Elect.*, vol. 65, no.1, pp. 749–759, Jan. 2018.
- [16] Y. Yang, S. S. Ho, S. C. Tan, and S. Y Hui, “Small-signal model and stability of electric springs in power grids,” *IEEE Trans. Smart Grid*, vol. 9, no. 2, pp. 857–865, Mar. 2018.
- [17] C. Wang, Y. Mi, Y. Fu, and P. Wang, “Frequency control of an isolated micro-grid using double sliding mode controllers and disturbance observer,” *IEEE Trans. Smart Grid*, vol. 9, no. 2, pp. 923–930, Mar. 2018.
- [18] G. Benysek, J. Bojarski, R. Smolenski, M. Jarnut, and S. Werminski, “Application of stochastic decentralized active demand response (DADR) system for load frequency control,” *IEEE Trans. Smart Grid*, vol. 9, no. 2, pp. 1055–1062, Mar. 2018.
- [19] Z. Miao, L. Fan, “A novel multi-agent decision making architecture based on dual’s dual problem formulation,” *IEEE Trans. Smart Grid*, vol. 9, no. 2, pp. 1150–1160, Mar. 2018.

- [20] S. Liu, P. X. Liu, “Distributed model-based control and scheduling for load frequency regulation of smart grids over limited bandwidth networks,” *IEEE Trans. Ind. Informat.*, vol. 14, No. 5, May. 2018.
- [21] M. Ashabani, and H. B. Gooi, “Multiobjective automated and autonomous intelligent load control for smart buildings,” *IEEE Trans. Power Syst.*, vol.33, no.3, pp. 2778–2891, May. 2018.
- [22] A. Tani, M. B. Camara, Member, IEEE, and B. Dakyo, “Energy management based on frequency approach for hybrid electric vehicle applications: fuel-cell/lithium-battery and ultracapacitors,” *IEEE Trans. Vehic. Tech.*, vol.61, no.8, pp.3375 –3386, Oct. 2012.
- [23] C. T. Li, C. Ahn, H. Peng, and J. Sun, “Synergistic control of plug-in vehicle charging and wind power scheduling,” *IEEE Trans. Power Syst.*, vol.28, no.2, pp. 1113–1121, May. 2013.
- [24] J. Tan, and L. Wang, “Integration of plug-in hybrid electric vehicles into residential distribution grid based on two-layer intelligent optimization,” *IEEE Trans. Smart Grid*, vol. 5, no. 4, pp. 1774–1784, Jul. 2014.
- [25] M. Bayat, K. Sheshyekani, and A. Rezaadeh, “A unified framework for participation of responsive end-user devices in voltage and frequency control of the smart grid,” *IEEE Trans. Power Syst.*, vol.30, no.3, pp. 1369–1379, May. 2015.
- [26] H. N. T. Nguyen, C. Zhang, and J. Zhang, “Dynamic demand control of electric vehicles to support power grid with high penetration level of renewable energy,” *IEEE Trans. Transp. Electrifi.*, vol. 2, no. 1, pp. 66–75, Mar. 2016.
- [27] S. Falahati, S. A. Taher, M. Shahidehpour, “Smart deregulated grid frequency control in presence of renewable energy resources by EVs charging control,” *IEEE Trans. Smart Grid*, vol. 9, no. 2, pp. 1073–1085, Mar. 2018.
- [28] B. Cheng, W. B. Powell, “Co-optimizing battery storage for the frequency regulation and energy arbitrage using multi-scale dynamic programming,” *IEEE Trans. Smart Grid*, vol. 9, no. 2, pp. 1997–2005, Mar. 2018.
- [29] L. Jiang, W. Yao, Q. H. Wu, J. Y. Wen, and S. J. Cheng, “Delay-dependent stability for load frequency control with constant and time-varying delays,” *IEEE Trans. on Power Syst.*, vol. 27, no. 2, pp. 932–941, May. 2012.

- [30] C. Zhao, U. Topcu, Member, IEEE, and S. H. Low, “Optimal load control via frequency measurement and neighborhood area communication,” *IEEE Trans on Power Syst.*, vol. 28, no. 4, pp. 3576–3587, Nov. 2013.
- [31] S. Liu, X. P. Liu, and A. El. Saddik. Modeling and distributed gain scheduling strategy for load frequency control in smart grids with communication topology changes. *ISA Transactions* 53(2014) 454–461.
- [32] Y. W. Law, T. Alpcan, and M. Palaniswami, “Security games for risk minimization in automatic generation control,” *IEEE Trans on Power Syst.*, vol. 30, no. 1, pp. 223–233, Jan. 2015.
- [33] V. P. Singh, N. Kishor, and P. Samuel, “Load frequency control with communication topology changes in smart grid,” *IEEE Trans. Ind. Informat.*, vol. 12, No. 5, Oct. 2016.
- [34] Y. Liu, Z. Qu, H. Xin, and D. Gan, “Distributed real-time optimal power flow control in smart grid,” *IEEE Trans on Power Syst.*, vol. 32, no. 5, pp. 3403–3414, Sep. 2017.
- [35] P. Ojaghi and M. Rahmani, “LMI-based robust predictive load frequency control for power systems with communication delays,” *IEEE Trans on Power Syst.*, vol. 32, no. 5, pp. 4091–4100, Sep. 2017.
- [36] C. Peng, J. Li, and M. Fei, “Resilient event-triggering h_∞ load frequency control for multi-area power systems with energy-limited dos attacks,” *IEEE Trans on Power Syst.*, vol. 32, no. 5, pp. 4110–4118, Sep. 2017.
- [37] F. Yang, J. He, and D. Wang, “New stability criteria of delayed load frequency control systems via infinite-series-based inequality,” *IEEE Trans. Ind. Informat.*, vol. 14, no. 1, pp. 231–240, Jan. 2018.
- [38] P. Babahajiani, Q. Shafiee, and H. Bevrani, “Intelligent demand response contribution in frequency control of multi-area power systems,” *IEEE Trans on Smart Grid*, vol. 9, no. 2, pp. 1282–1291, Mar. 2018.
- [39] G. S. Ledva, E. Vrettos, S. Mastellone, G. Andersson, and J. L. Mathieu, “Managing communication delays and model error in demand response for frequency regulation,” *IEEE Trans on Power Syst.*, vol. 33, no. 2, pp. 1299–1308, Mar. 2018.
- [40] H. Saadat, *Power System Analysis*. New York, NY, USA: McGraw-Hill, 1999.

- [41] H. Bevrani, *Robust Power System Frequency Control*. New York, NY, USA: Springer, 2004.
- [42] I. Lampropoulos, N. Baghină, W. L. Kling, and P. F. Ribeiro, “A predictive control scheme for real-time demand response applications,” *IEEE Trans on Smart Grid*, vol. 4, no. 4, pp. 2049–2060, Dec. 2013.
- [43] X. Wang, Q. Zhao, B. He, Y. Wang, J. Yang, X. Pan, “Load frequency control in multiple microgrids based on model predictive control with communication delay,” *The Journ. of Engg.*, vol. 2017, Iss. 13, pp. 1851–1856, Oct. 2017.
- [44] S. Prasad, S. Purwar, N. Kishor, “H-infinity based non-linear sliding mode controller for frequency regulation in interconnected power systems with constant and time-varying delays,” *IET Gener. Transm. Distrib.*, vol. 10, Iss. 11, pp. 2771–2784, Apr. 2016.

APPENDIX

MATLAB code for finding stability of closed loop system

```
A = [-0.116    0.081    0    0    0    0    -0.081    0    0;
      0    -0.111    0.111    0    0    0    0    0    0;
     -4    0    4    0    0    0    0    0    0;
      0    0    0    -0.110    0.077    0    -0.077    0    0;
      0    0    0    0    -0.111    0.111    0    0    0;
      0    0    0    4    0    -4    0    0    0;
      1    0    0    -1    0    0    0    0    0;
      8    0    0    0    0    0    1    0    0;
      0    0    0    8    0    0    -1    0    0]
```

```
B = [0  0;
      0  0;
      4  0;
      0  0;
      0  0;
      0 -4;
      0  0;
      0  0;
      0  0]
```

```

P = [64  0  0  0  0  0  0  8  0  0;
      0  0  0  0  0  0  0  0  0  0;
      0  0  0  0  0  0  0  0  0  0;
      0  0  0  64  0  0 -8  0  0  0;
      0  0  0  0  0  0  0  0  0  0;
      0  0  0  0  0  0  0  0  0  0;
      8  0  0 -8  0  0  2  0  0  0;
      0  0  0  0  0  0  0  0  1  0;
      0  0  0  0  0  0  0  0  0  1]

```

```

G = [1  0;
      0  1]

```

```
T = care(A,B,P,G)
```

```
K = inv(G)*B'*T
```

```
N = A-B*K
```

```
Eig(T)
```

```
Eig(A)
```

```
Eig(N)
```

T = 1.0e+03 *

2.9143	0.3521	0.0080	-1.6084	-0.2030	-0.0050	0.3196	0.0909	-0.0279
0.3521	0.0632	0.0016	-0.0850	-0.0142	-0.0004	0.0003	0.0104	-0.0014
0.0080	0.0016	0.0005	-0.0016	-0.0003	-0.0000	-0.0001	0.0002	-0.0000
-1.6084	-0.0850	-0.0016	5.0992	0.5942	0.0144	-1.1366	-0.0027	0.1264
-0.2030	-0.0142	-0.0003	0.5942	0.0846	0.0021	-0.1367	0.0009	0.0109
-0.0050	-0.0004	-0.0000	0.0144	0.0021	0.0001	-0.0033	0.0000	0.0002
0.3196	0.0003	-0.0001	-1.1366	-0.1367	-0.0033	0.2675	0.0002	-0.0258
0.0909	0.0104	0.0002	-0.0027	0.0009	0.0000	0.0002	0.0051	-0.0001
-0.0279	-0.0014	-0.0000	0.1264	0.0109	0.0002	-0.0258	-0.0001	0.0056

K =

31.9948	6.3984	2.1637	-6.5244	-1.2077	-0.0309	-0.5361	0.9944	-0.1057
19.8537	1.4352	0.0309	-57.5301	-8.4416	-0.2114	13.3042	-0.1057	-0.9944

N =

-0.1160	0.0810	0	0	0	0	-0.0810	0	0
0	-0.1110	0.1110	0	0	0	0	0	0
-131.9791	-25.5934	-4.6547	26.0978	4.8308	0.1235	2.1445	-3.9776	0.4229
0	0	0	-0.1100	0.0770	0	-0.0770	0	0
0	0	0	0	-0.1110	0.1110	0	0	0
79.4148	5.7406	0.1235	-226.1205	-33.7662	-4.8457	53.2167	-0.4229	-3.9776
1	0	0	-1	0	0	0	0	0
8.0000	0	0	0	0	0	1.0000	0	0
0	0	0	8.0000	0	0	-1.0000	0	0

Eigen values T = 1.0e+03 *

0.0000

0.0004

0.0005

0.0012

0.0015

0.0176

0.0286

2.1360

6.2544

Eigen values A = 0.0000 + 0.0000i

0.0000 + 0.0000i

3.9979 + 0.0000i

-3.9977 + 0.0000i

-0.2002 + 0.0091i

-0.2002 - 0.0091i

0.0026 + 0.0000i

-0.0251 + 0.0445i

-0.0251 - 0.0445i

Eigen values N = $-3.9979 + 0.0000i$

$-3.9978 + 0.0000i$

$-0.2061 + 0.4092i$

$-0.2061 - 0.4092i$

$-0.2555 + 0.2916i$

$-0.2555 - 0.2916i$

$-0.2857 + 0.0595i$

$-0.2857 - 0.0595i$

$-0.4582 + 0.0000i$

PLAGIARISM REPORT

Rushil thesis

ORIGINALITY REPORT

11% **7%** **10%** %
SIMILARITY INDEX INTERNET SOURCES PUBLICATIONS STUDENT PAPERS

PRIMARY SOURCES

- 1** Pouya Babahajiani, Qobad Shafiee, Hassan Bevrani. "Intelligent Demand Response Contribution in Frequency Control of Multi-Area Power Systems", IEEE Transactions on Smart Grid, 2018
Publication <1%
- 2** Bunker, Kaitlyn J., and Wayne W. Weaver. "Microgrid frequency regulation using wind turbine controls", 2014 Power and Energy Conference at Illinois (PECI), 2014.
Publication <1%
- 3** Kai Liao, Yan Xu. "A Robust Load Frequency Control Scheme for Power Systems Based on Second-Order Sliding Mode and Extended Disturbance Observer", IEEE Transactions on Industrial Informatics, 2017
Publication <1%
- 4** K. Ratna Jyothy, Ch. Padmanabha Raju, R. Srinivasarao. "Simulation studies on WTG-FC-battery hybrid energy system", 2017 <1%